

Jupiter's Magnetosphere: Plasma Sources and Transport

Scott J. Bolton¹ · Fran Bagenal² · Michel Blanc³ · Timothy Cassidy⁴ ·
Emmanuel Chané⁵ · Caitriona Jackman⁶ · Xianzhe Jia⁷ · Anna Kotova⁸ ·
Norbert Krupp⁸ · Anna Milillo⁹ · Christina Plainaki⁹ · H. Todd Smith¹⁰ ·
Hunter Waite¹

Received: 17 March 2015 / Accepted: 8 July 2015 / Published online: 7 October 2015
© Springer Science+Business Media Dordrecht 2015

1 Introduction

Jupiter's plasma environment is one of the most interesting plasma laboratories in our solar system. Studying the plasma sources and sinks, as well as understanding the configuration and dynamics of the Jovian magnetosphere is key to the understanding of similar astrophysical systems in our galaxy. The study of Jupiter's plasma environment can be used as a template for exoplanets as well as examples of acceleration processes in protoplanetary discs.

The Jovian system is a world of superlatives: it is built around the largest planet in our solar system, more than 10 times bigger than the Earth (1 Jupiter radius (R_J) = 71492 km). Jupiter has the strongest magnetic field of all planets (its magnetic moment is 20000 times larger than Earth's, its surface magnetic field is 14 times larger compared to Earth), the largest magnetosphere (the radius of the terminator cross section is about $150R_J$) and the

✉ S.J. Bolton
sbolton@swri.edu

¹ Southwest Research Institute, San Antonio, TX, USA

² University of Colorado, Boulder, CO, USA

³ IRAP, CNRS-Université Paul Sabatier, Toulouse Cedex 4, France

⁴ LASP, University of Colorado, Boulder, CO, USA

⁵ Center for Mathematical Plasma Astrophysics, KU Leuven, Leuven, Belgium

⁶ Department of Physics and Astronomy, University of Southampton, Southampton, UK

⁷ Department of Atmospheric, Oceanic, and Space Sciences, University of Michigan, Ann Arbor, MI, USA

⁸ Max-Planck-Institut für Sonnensystemforschung, Göttingen, Germany

⁹ Institute of Space Astrophysics and Planetology, INAF, Rome, Italy

¹⁰ Applied Physics Laboratory, Johns Hopkins University, Laurel, MD, USA

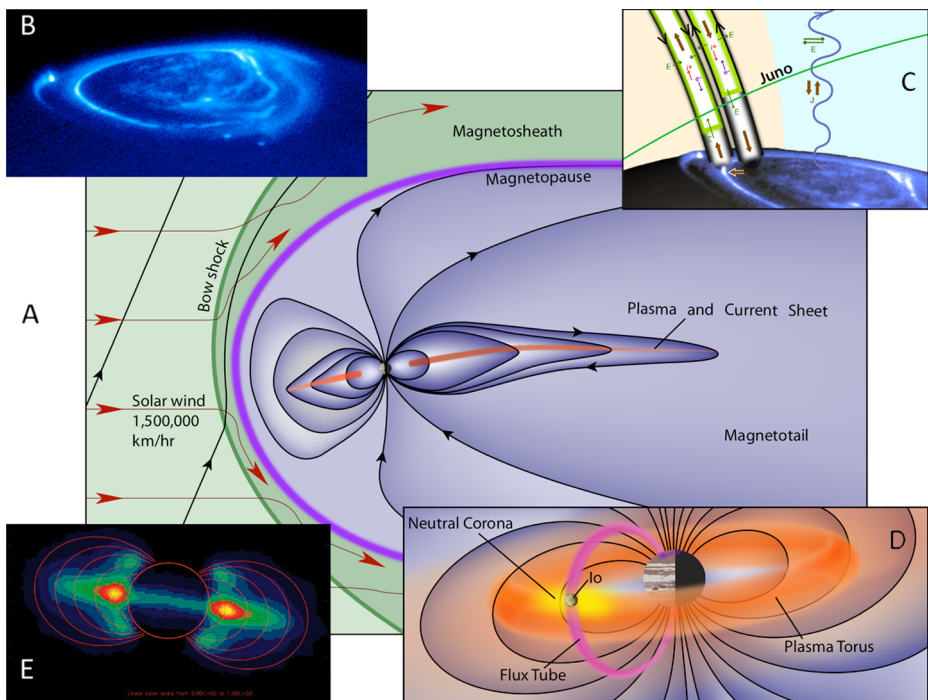


Fig. 1 (A) The magnetosphere of Jupiter extends 63–92 Jovian radii in the direction towards the Sun, with a tail that stretches beyond the orbit of Saturn > 4 AU, and occupies a volume over a thousand times that of the Sun. (B) Intense auroral emissions are signatures of the coupling between the planet and the magnetospheric plasmas. (C) Terrestrial experience suggests that there are regions within a few radii of the planet where the aurora-generating particles are excited. The *Juno* spacecraft will fly through these regions. (D) The magnetosphere is dominated by a ~1 ton/s source of plasma from Io's volcanic gases that forms a toroidal cloud around Jupiter. (E) Close to the planet are strong radiation belts comprising energetic (MeV) electrons that emit synchrotron emission. From Bagenal et al. (2014)

strongest radiation belts (see Fig. 1). Jupiter's auroral power is about 100 times stronger than at Earth. Jupiter is surrounded by 67 moons, the largest number of all planets. The moon Io is the body with the strongest volcanic activity in our solar system, Ganymede is the biggest moon of all in the heliosphere and the only moon with its own intrinsic magnetic field forming a unique mini-magnetosphere within the large Jovian magnetosphere.

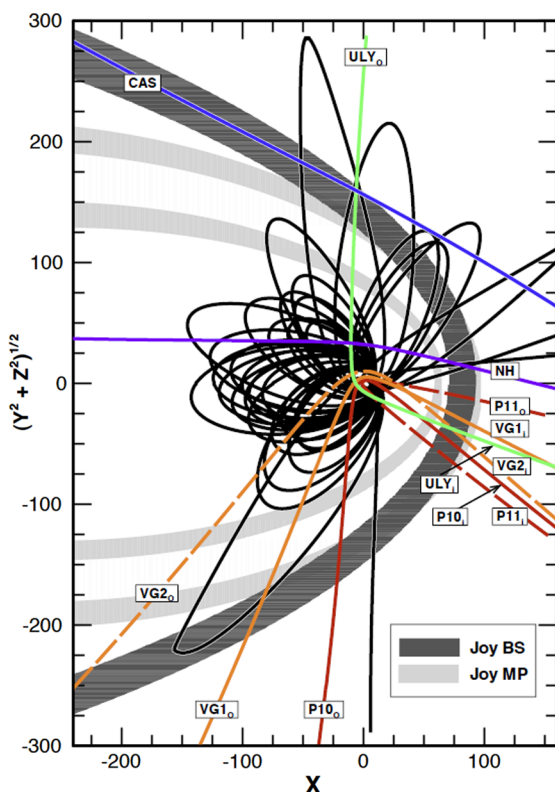
Jupiter has been visited by a total of eight spacecraft in the last 40 years (see Table 1 and Fig. 2), but thus far the only dedicated orbiter has been the Galileo spacecraft, which orbited between 1995 and 2003 and is the source of most of our current knowledge about the Jovian system. Most recently (2006–2007), the New Horizons spacecraft traversed the Jovian tail to distances greater than $2500R_J$ on its way to Pluto. The next chance to explore Jupiter will be with the arrival of the Juno mission in 2016 (Bolton 2010; Bolton et al. 2015) to be followed by the JUICE mission in 2030 (Grasset et al. 2013).

The measurements from these missions and telescopes have been used as input for global simulations of the entire magnetosphere as well as to derive new models of the magnetic field and the plasma environment. Based on these data and simulations our current view of the Jovian plasma environment is described below.

Table 1 Spacecraft exploration of the Jovian system

Spacecraft that encountered Jupiter	Year(s)	Type
Pioneer 10 (P10)	1973	Flyby
Pioneer 11 (P11)	1974	Flyby
Voyager 1 (VG1)	1979	Flyby
Voyager 2 (VG2)	1979	Flyby
Ulysses (ULY)	1992	Flyby
Galileo (GLL)	1995–2003	Orbiter
Cassini (CAS)	2000/2001	Flyby
New Horizons (NH)	2007	Flyby

Fig. 2 Trajectories of the spacecraft that have visited Jupiter's magnetosphere (Vogt 2012). The shaded areas indicate the minimum and maximum distances of the magnetopause (MP, light gray) and bow shock (BS, dark gray) after Joy et al. (2002)



The pre-Galileo understanding of the Jovian magnetosphere is presented in Dessler's (1983) book *Physics of the Jovian Magnetosphere* and the advances made by the *Ulysses* and *Galileo* missions are reviewed in seven chapters of *Jupiter: The Planet, Satellites and Magnetosphere* (edited by Bagenal et al. 2004). Bagenal et al. (2014) reviewed the Jovian magnetosphere in anticipation of Juno's arrival in 2016, while the Jovian tail was reviewed by Krupp et al. (2015).

2 Global Configuration

The classical scale of a planet's magnetosphere, namely the Chapman-Ferraro radius R_{CF} , as derived by Chapman and Ferraro (1930), comes from a simple pressure balance between the ram pressure of the solar wind (ρV^2)_{sw} and the magnetic pressure of a dipole field ($B^2 2\mu_0$) assumed to represent the planetary magnetic field. This results in a weak variation in the dayside magnetopause distance R_{MP} such that $R_{MP} \propto (\rho V^2)_{sw}^{-1/6}$ (for a solar wind mass density $\rho_{sw} = m_p n_{sw}$ and speed V_{sw}). While this Chapman-Ferraro magnetopause distance works well for Earth (except during periods of extremely unusual solar wind conditions, see Chané et al. 2012), it underestimates the sizes of the giant planet magnetospheres, particularly Jupiter. If the pressure P of the charged particle populations inside the magnetosphere dominates over the local magnetic field pressure ($B^2 2\mu_0$), then $\beta = P/(B^2 2\mu_0) > 1$ and the particle pressure inflates and stretches out the magnetic field, generating strong currents in the equatorial plasma disk. In addition, the centrifugal force associated with the plasma rotating around the planet also stretches the magnetosphere. Figure 1 illustrates how the substantial internal plasma pressure as well as the centrifugal force at Jupiter expands the magnetosphere well beyond that of a dipole internal field. At Jupiter, values of β greater than unity are found beyond $\sim 15R_J$, increasing to $\beta > 100$ by $45R_J$ (Mauk et al. 2004). In addition to the plasma pressure dominating the magnetic pressure, the radial profile of plasma pressure is considerably flatter than the $R^{-1/6}$ variation in magnetic pressure for a dipole field. It is the high plasma pressure in the plasma disk as well as the centrifugal force that doubles the scale of Jupiter's magnetosphere from the dipolar stand-off distance of $\sim 42R_J$ to over $90R_J$.

Careful statistical analysis (combined with modeling) of how the magnetopause standoff distance at Jupiter varies with solar wind conditions by Joy et al. (2002) revealed a bimodal distribution with high probabilities at 63 and $92R_J$. Furthermore, the observed magnetopause locations indicate a variation in R_{MP} with solar wind ram pressure $R_{MP} \propto (\rho V^2)_{sw}^{-\alpha}$ where α is found to be between $1/3.8$ and $1/5.5$, a stronger function than for a dipole (Slavin et al. 1985; Huddleston et al. 1997; Joy et al. 2002; Alexeev and Belenkaya 2005). A factor 10 increase in ram pressure at Earth reduces R_{MP} to 70 % of the nominal value, while at Jupiter a tenfold variation in solar wind pressure, often observed at 5 AU (Jackman and Arridge 2011; Ebert et al. 2014), causes the dayside magnetopause to move by a factor of ~ 2 .

The overall configuration of the Jovian system has been very well described in the literature (see review articles from Khurana et al. 2004 and from Krupp et al. 2004b) and consists of an inner, middle and an outer magnetosphere, with transitions between those segments at approximately 10 – $15R_J$ and at 40 – $60R_J$. The major energy source of the system is derived from its fast rotation (with a rotation period of about 10 hours) and the major particle source is sputtered from Io's atmosphere and surface. Io is orbiting deep within the magnetosphere at $5.9R_J$. The magnetic dipole axis is tilted about 10° from the rotation axis of the planet.

The inner magnetosphere ($< 15R_J$) close to the planet is the region of trapped charged particles on dipolar-like field lines. This is the region of the harshest radiation belts in our solar system where electrons and ions reach energies of tens of MeV, with very high intensities (reviewed by Woodfield et al. 2014; Bolton et al. 2004). The sources of these populations include both galactic cosmic rays and radially inward drifting particles originating in the outer magnetosphere (see description below). The inner magnetosphere also includes the ring system of the planet (related to the moons Amalthea and Thebe) and the Galilean moon Io which is the major plasma source of the system. Gases escaping from Io's atmosphere form a neutral cloud extending along Io's orbit around Jupiter. Ionization of this neutral cloud produces a torus of plasma that emits over a terawatt of line emissions, mostly in

the UV (reviewed by Thomas et al. 2004) powered by ion pickup in the rapidly rotating system.

The middle magnetosphere of Jupiter ($15 < r < 60R_J$) is the region where the magnetic field stretches radially and significantly deviates from a dipole. Caused by the mass loading of the magnetic field lines with heavy ions from Io and due to the centrifugal forces in the rapidly rotating environment the entire magnetosphere is radially stretched forming a magnetodisc and associated current sheet close to the equatorial plane. Electrical currents flowing along the magnetic field couple the magnetodisc to the planet and transfer momentum from the neutral atmosphere to the magnetodisc. This momentum transfer is very efficient close to the planet and forces the plasma to rigidly corotate. However, farther from Jupiter, this coupling is not strong enough to accelerate the plasma to rigid corotation: the plasma sub-corotates (its angular velocity is lower than Jupiter's angular velocity). The region of the “corotation breakdown” is a function of local time and a function of time (see Bonfond et al. 2012). It is this current system which is responsible for the main auroral emission (see Hill 2001; Cowley and Bunce 2001) where mainly keV electrons are accelerated downward into the polar regions, hitting atmospheric particles and emitting radiation across the spectrum, from x -rays, UV and visible to IR and radio (reviewed by Clarke et al. 2004).

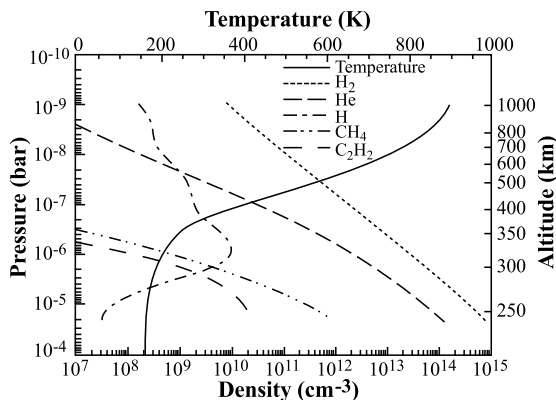
The outer magnetosphere beyond $40\text{--}60R_J$ is the region where the magnetic field lines are stretched further, until the magnetopause on the dayside, or several $1000R_J$ down the Jovian magnetotail on the nightside. While the Galileo trajectories covered only distances as far out as $150R_J$ near local midnight, the New Horizons spacecraft has sampled the coherent Jovian magnetotail in situ to distances from $1600R_J$ (McNutt et al. 2007) to $2500R_J$. However, observations from the Voyager spacecraft suggest that the Jovian tail can stretch even as far as the orbit of Saturn (Kurth et al. 1982; Scarf et al. 1982), which would make the Jovian magnetosphere by far the largest coherent structure in our solar system (except for the heliosphere itself).

The whole system is fed by plasma sources that predominately come from inside the magnetosphere with external contributions. The volcanic moon Io is the strongest internal source, with minor contributions from the moon Europa and possibly other moons as well as Jupiter's ionosphere. Embedded in the inner Jovian magnetosphere, the icy moons experience a strong interaction with their surrounding plasma. Data from Galileo showed that these moons are continuously irradiated by energetic ions (H^+ , C^{n+} , O^{n+} and S^{n+}) and electrons in the energy range from keV to MeV (Cooper et al. 2001; Paranicas et al. 2002). The effects of this intense irradiation on ice are the main drivers of the generation of tenuous atmospheres around these bodies and could be of crucial importance in generating the conditions of the ocean below the icy crust (Chyba 2000). However, the details of the surface processes and their impact on the environment are poorly known. External plasma sources for the Jovian magnetosphere are the solar wind and galactic cosmic rays. The details will be described in subsequent sections. We will first address Jupiter's atmosphere and ionosphere, followed by Io and the Io plasma torus. We then address Europa and Ganymede and finally the solar wind, and a general discussion on transport mechanisms.

3 Atmosphere and Ionosphere

Unlike the Earth and inner terrestrial planets, Jupiter does not have a solid surface. Altitude scales are generally referred to a reference pressure level, which is generally accepted to be the 1 bar level. This pressure level corresponds to a radial distance of about 71492 km from

Fig. 3 A model of Jupiter's atmosphere, showing neutral gas densities and temperatures (from Schunk and Nagy 2009, courtesy of Tariq Majeed)



the center of Jupiter at the equator. Note that Jupiter, as all outer planets, is oblate due to the planet's rapid rotation rate. The atmosphere of Jupiter consists predominantly of molecular hydrogen and some lesser amounts of helium and atomic hydrogen. In the lower atmosphere CH_4 and other hydrocarbons are also present as minor constituents. The latest estimate of the thermospheric temperature at Jupiter is about 900 K. However, this value is rather uncertain. At present, the energy sources responsible for this relatively high temperature have not been established; candidate sources include Joule heating, gravity wave dissipation, and precipitating particle energy deposition. The latest estimates of the densities and the neutral gas temperature at Jupiter are shown in Fig. 3 based on a model of pressure and altitude profiles of the major neutrals in Jupiter's atmosphere.

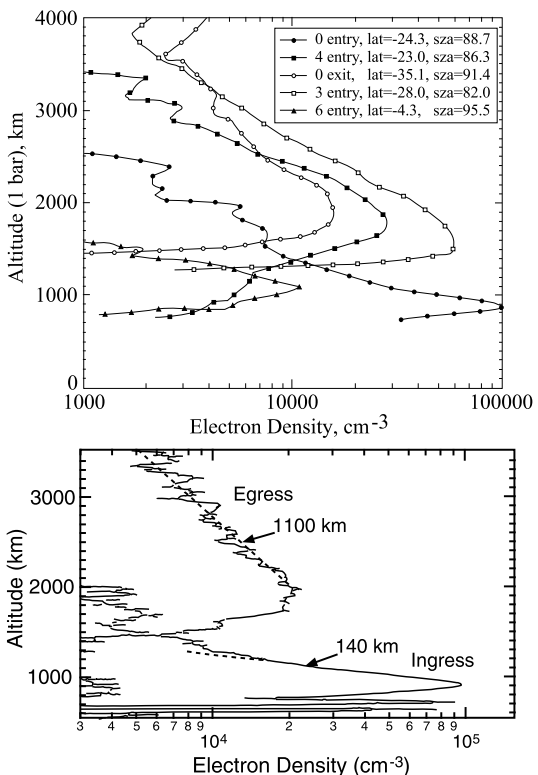
The presently available direct information regarding the ionosphere of Jupiter is based on the Pioneer 10 and 11, Voyager 1 and 2 and Galileo radio occultation measurements. There is no direct information available concerning ion composition or plasma temperatures in Jupiter's ionosphere; our limited understanding is based on model calculations. Given that Jupiter's upper atmosphere consists mainly of molecular hydrogen, the major primary ion, formed by either photoionization or particle impact ionization, is H_2^+ . In the equatorial and low to mid latitudes the electron-ion pair production is mainly due to photoionization, while at high latitudes impact ionization by precipitating particles is believed to become very important. The actual equilibrium concentration of the major primary ion, H_2^+ , is likely to be very small because it undergoes rapid charge transfer reaction with neutral molecular hydrogen, resulting in H_3^+ , which is believed to be a major ion and which is eventually lost by dissociative recombination with an electron, as indicated below:



The presence of H_3^+ in Jupiter's ionosphere has been confirmed by ground-based measurements using the NASA Infrared Telescope Facility (IRTF) on Mauna Kea, Hawaii (Stallard et al. 2002). They estimated that the nighttime vibrational temperature is somewhere between 940 and 1065 K and the column density is of the order of $1 \times 10^{16} \text{ m}^{-2}$.

Protons, H^+ are created at high altitudes by either the direct ionization of neutral atomic hydrogen or by the dissociative ionization of molecular hydrogen. H^+ can only recombine directly via radiative recombination, which is extremely slow. It was suggested years ago (McElroy 1973) and discussed in Chap. 2 (2.1.2b) (Seki et al. 2015) that it can be lost via

Fig. 4 Galileo radio occultation measurements of ionospheric electron densities (above) (from Schunk and Nagy 2009, courtesy of A.J. Kliore)



charge exchange with the fraction of molecular hydrogen which is in a vibrational state of 4 or higher. The uncertainty associated with the loss process of H^+ leaves open the question of the identity of the major ion near the ionospheric peak as a function of latitude. There are no measurements that constrain the vibrational distribution of molecular hydrogen, but some model calculations do indicate a significant population in the higher excited states (Cravens 1987; Hallett et al. 2005). Direct photoionization of hydrocarbon molecules at lower altitudes can lead to a relatively thin layer around 300 km (Kim and Fox 1994).

Figure 4 shows electron density profiles obtained by the radio occultation technique from the Galileo spacecraft. The top figure shows examples of egress and ingress for multiple latitudes. The observed peak electron densities are in the range of 10^4 to 10^5 cm^{-3} . By the nature of the encounter geometries all these results are very close to the terminator, thus representing similar solar zenith angles. There is great variability among the observed density profiles in the top panel and there seems to be no clear latitude dependence. The lower panel of Fig. 4 compares the two extreme cases of the altitude of the peak electron density and the topside scale height. These examples illustrate significantly different atmospheric profiles; the higher altitude peak is associated with a greater scale height. These differences may be the result of different major ionization source or loss mechanisms or different chemistries. A number of one and multi-dimensional models have been published to date (Majeed and McConnnell 1991; Bouger et al. 2005; Millward et al. 2005), but none of these models have provided any clear explanation of these very significant variations.

The ionosphere may be a source of plasma for the magnetosphere. At Jupiter, the most convincing evidence comes from Hamilton et al. (1981) who report fluxes in the Jovian magnetosphere of He^+ and H_3^+ ions, which most likely come from Jupiter's ionosphere. The outflow of ionospheric plasma was proposed by Nagy et al. (1986) and estimated to be 2×10^{28} ions/s which is comparable in number density to the iogenic source (see next section) but, assuming the composition is mostly protons, the mass would be only 35 kg/s.

4 Io and the Plasma Torus

The magnetosphere of Jupiter is greatly influenced by strong internal sources of neutral particles and of plasma located deep inside the magnetosphere, i.e. the Galilean moons Io, and Europa, and to a lesser extent Ganymede and Callisto (see review by Thomas et al. 2004). While Io's atmosphere is dominated by sulfur dioxide (SO_2), Europa's atmosphere mostly contains molecular oxygen (O_2), but also molecular hydrogen (H_2) at higher altitudes. Particles from these atmospheres are constantly ejected into the Jovian magnetosphere, either directly as gas, or as plasma. Most of the neutral particles present in the magnetosphere stem from either charge-exchange processes or elastic collisions between the heavy ions in the magnetosphere and the atmosphere of Io or Europa. These neutral particles are then on a Keplerian orbit around the planet, forming the Io and Europa neutral clouds. These extended neutral gas clouds experience ionization processes and charge exchange collisions, making them the dominant source of plasma. The Io and Europa atmospheres are also a direct source of plasma, because their neutral particles are subject to electron impact (and to a lesser extent photo-) ionization, and to charge exchange collisions with the magnetospheric plasma. Once these particles are charged they are accelerated by the Lorentz force, and start to corotate around the planet (i.e. they feel the effect of Jupiter's rotating magnetic field). When charge exchange occurs, the charged particles (which move at approximately the corotation speed) become neutralized and escape the torus.

Compared with the local plasma, which is nearly corotating with Jupiter at 74 km/s, the neutral atoms are moving slowly, close to Io's orbital speed of 17 km/s. When a neutral atom becomes ionized (largely via electron impact) it becomes subject to the ambient Jovian corotation electric field, resulting in a gyromotion of 57 km/s. Thus, new S^+ and O^+ ions gain 540 eV and 270 eV in gyro-energy, respectively. The new "pick-up" ion is also accelerated up to the bulk speed of the surrounding plasma by the magnetic Lorentz force. The necessary momentum comes from Jupiter's upper atmosphere and ionosphere via field aligned currents—the Jovian rotation being the ultimate source of momentum and energy for these (and most) processes in the magnetosphere. About one-third to one-half of the neutral atoms are ionized to produce additional fresh plasma, while the rest are lost via reactions in which a neutral atom exchanges an electron with a torus ion. When neutralized, the previously charged, corotating particle is no longer confined by the magnetic field and, since the corotation speed is well above the gravitational escape speed from Jupiter, flies off as an energetic neutral atom. This charge-exchange process adds gyro-energy to the ions and extracts momentum from the surrounding plasma, but it does not add more plasma to the system (even though it can add or remove mass to the system in case of asymmetric charge-exchange: when the neutral particle and the ion do not have the same mass).

Smyth and Marconi (2006) developed a model of the neutral clouds in the Jovian magnetosphere. The longitudinally-averaged column density of the neutral particles that they obtained is displayed in Fig. 5. This figure shows that close to Jupiter (less than $\sim 7.5R_J$) the majority of the neutral particles are from Io, while farther away (beyond $\sim 7.5R_J$) most

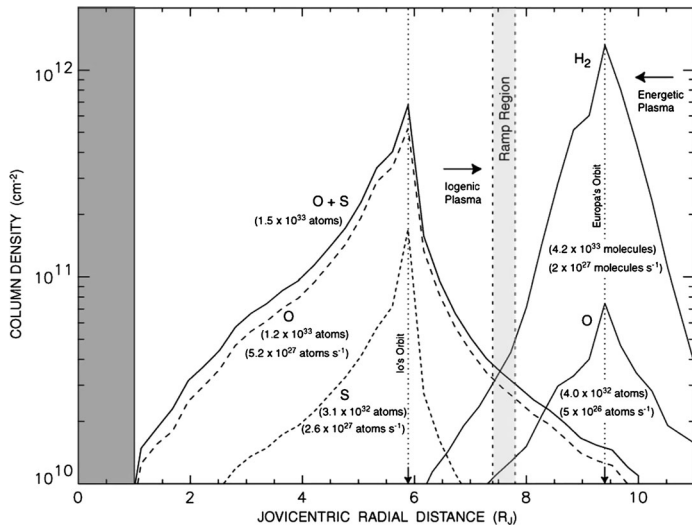


Fig. 5 Longitudinally-averaged radial column density of the neutral clouds of Io and Europa (from Smyth and Marconi 2006)

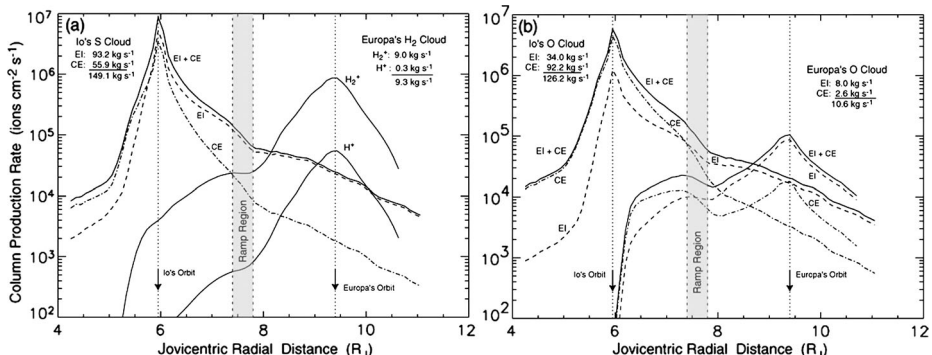


Fig. 6 Longitudinally-averaged column production of pickup ions generated by Io's and Europa's neutral clouds (from Smyth and Marconi 2006)

of them come from Europa. If one just counts the total number of surviving neutral particles in these clouds, the molecular hydrogen emanating from Europa (4.2×10^{33} molecules) is larger than the combined number of oxygen and sulfur atoms around the Io region (1.5×10^{33} atoms). The mass-loading associated with Io's and Europa's tori is shown in Fig. 6. According to Smyth and Marconi's (2006) model, the largest source of plasma is, by far, Io (particularly the extended neutral cloud), with a plasma production rate of $\sim 250 \text{ kg/s}$, while Europa's atmosphere and neutral cloud only generate $\sim 22\text{--}27 \text{ kg}$ of plasma per second. Even though the number density of molecular hydrogen at Europa's orbit is higher than the density of sulfur atoms and oxygen atoms at the orbit of Io, the mass-loading rate at the orbit of Europa is more than an order of magnitude lower than at the orbit of Io. This is because: (1) the oxygen and sulfur atoms are heavier than molecular hydrogen, and (2) the

electron temperature is much higher at smaller radial distances, meaning that electron impact ionization is more efficient at the orbit of Io.

Strong centrifugal forces confine the plasma near the equator. Thus, the densest plasma ($\sim 2000 \text{ cm}^{-3}$) forms a torus around Jupiter near the orbit of Io. A lighter population of H⁺ ions (with a relative concentration of a few % and a temperature of a few 10s eV), less confined near the equator, has been inferred from radio (decametric, DAM) measurements (Zarka et al. 2001). The Io plasma torus has a total mass of ~ 2 megaton, which would be replenished by a source of $\sim 1 \text{ ton/s}$ in ~ 23 days. Multiplying by the typical energy of the ions ($T_i \sim 60 \text{ eV}$) and electrons ($T_e \sim 5 \text{ eV}$), we obtain $\sim 6 \times 10^{17} \text{ J}$ for the total thermal energy of the torus. The observed UV power is about 1.5 TW, emitted via more than 50 ion spectral lines, most of which are in the EUV. This emission would drain all the energy of the torus electrons in $\sim 7 \text{ h}$. Ion pickup replenishes energy, and Coulomb collisions feed the energy from ions to electrons but not at a sufficient rate to maintain the observed emissions. A source of additional energy, perhaps mediated via plasma waves, seems to be supplying hot electrons and a comparable amount of energy as ion pickup. The 20–80 day time scale (equivalent to 50–200 rotations) for the replacement of the torus indicates surprisingly slow radial transport that maintains a relatively strong radial density gradient.

It should be noted that these mass-loading rates vary on time scales of months to years. For the Io torus, Bagenal and Delamere (2011) estimated that at the time of Voyager 1 in March 1979 the neutral source and the plasma source were 800 kg/s and 260 kg/s, respectively. At the time of the Cassini flyby in September 2000, these sources were much higher: 3000 kg/s and 1400 kg/s, respectively. Bonfond et al. (2012) also argued that a major increase of the mass-loading rate happened in the spring of 2007, which had considerable repercussions for the configuration of the Jovian magnetosphere. These authors observed that the position of the main oval moved equatorward over a few months, which is consistent with an increased mass-loading rate.

As the Iogenic plasma moves outward, the conservation of angular momentum would suggest that the plasma should lose angular speed. In a magnetized plasma, however, electrical currents easily flow along magnetic fields and couple the magnetospheric plasma to Jupiter's flywheel. Hill (1979) argued that at some point the load on the ionosphere increases to the point where the coupling between the ionosphere and corotating atmosphere—manifested as the ionospheric conductivity—is not sufficient to carry the necessary current, causing the plasma to lag behind corotation. The main aurora is the signature of Jupiter's attempt to spin up its magnetosphere or, more accurately, Jupiter's failure to spin up its magnetosphere fully (see Cowley and Bunce 2001). The position of the corotation break-down, and thus the latitude of the main oval, depends on the mass-loading rate. Hill (1979), assuming that the magnetic field was a simple dipole, derived the following expression for the position of the corotation break-down:

$$R_0 = \sqrt[4]{\frac{2\pi\Sigma(\mu_0/4\pi M_p)^2}{\dot{M}}} \quad (4.1)$$

where Σ is the conductance of the ionosphere, μ_0 the permeability of free space, M_p the planetary magnetic moment, and \dot{M} the total rate of production and outward transport of plasma mass. Analytical models (Hill 1979; Cowley and Bunce 2001; Nichols and Cowley 2003) are very useful for understanding the dynamics of the magnetosphere, but being axisymmetric, they cannot account for local time asymmetries. To study the three-dimensional structure of the magnetosphere, global simulations are more appropriate (Miyoshi and Kusano 1997; Ogino et al. 1998; Walker et al. 2001; Fukazawa et al. 2005;

Moriguchi et al. 2008; Chané et al. 2013). For instance, Chané et al. (2013) have shown that the discontinuity of the main oval in the pre-noon sector (discovered by Radioti et al. 2008) was caused by an asymmetry in the pressure distribution, due to the interaction between the rotating plasma and the magnetopause. It is known that the mass-loading rate affects the position of the main oval, but does it influence the intensity of the main oval? Nichols and Cowley (2003), using their axisymmetric analytical model, showed that, if one assumes that the magnetic field in the magnetosphere is dipolar, the peak value of the field-aligned currents in the ionosphere does not depend on the mass-loading rate:

$$(j_{\parallel}/B)_{max} \approx 0.1076 \Sigma_P^* (\text{mho}) \text{ pA m}^{-2} \text{ nT}^{-1} \quad (4.2)$$

On the other hand, using a more realistic magnetic field (the current sheet magnetic field model, see Connerney et al. 1981; Edwards et al. 2001) they found that the peak value of the field-aligned currents depends weakly on the mass-loading rate:

$$(j_{\parallel}/B)_{max} \approx 2.808 (\Sigma_P^* (\text{mho})^{3.42} \dot{M} (10^3 \text{ kg/s})^{-0.71})^{1/2.71} \text{ pA m}^{-2} \text{ nT}^{-1} \quad (4.3)$$

Using this formula, one finds that if the mass-loading rate increases by an order of magnitude, the field-aligned current peak value decreases by less than a factor of two. However, Nichols and Cowley (2003) did not take into account the fact that the magnetic field could be affected by the mass-loading rate. This effect was included in Nichols (2011), where a magnetic field model similar to the one from Caudal (1986) was used. Depending on the assumption made in this model (namely whether the cold plasma density depends on the mass-loading rate or not) they found that the peak value of the field-aligned currents is correlated or anti-correlated with the mass-loading rate; and this remains, as of today, an open question.

The above models of corotation breakdown assume the coupling is limited by the ionospheric conductivity. Studies by Ergun et al. (2009) and Ray et al. (2010, 2012, 2014) point out that the rarefaction of plasma between the plasma sheet and the ionosphere leads to small-scale regions of parallel electric fields (“double-layers”) a few R_J above the ionosphere. They argue that the linear approximation to Knight’s current-voltage relation (Knight 1973) (for more detail see Seki et al. 2015) commonly assumed for ionosphere-magnetosphere coupling, breaks down and that the currents flowing between the two regions become saturated, modifying the coupling between the magnetosphere and ionosphere. The Juno spacecraft will fly through the polar regions of Jupiter’s magnetosphere with a suite of particles and fields instruments that will elucidate this key issue of magnetosphere-ionosphere coupling.

5 Europa

Europa is embedded in the radiation belt of Jupiter and it is not protected by an internal magnetic field; hence, it is subjected to energetic ion bombardment. The Jovian magnetospheric plasma, confined by Jupiter’s magnetic field, slightly subcorotates anticlockwise at ~ 100 km/s at the orbit of Europa (Kivelson et al. 2009). Since the orbital velocity of Europa is 14 km/s anticlockwise, the bulk plasma flow is constantly overtaking the satellite. Mauk et al. (2004) showed that the energy deposited on the icy satellites by magnetospheric particles is carried principally by the particles at energies above 10 keV.

As a consequence of this deposited energy, Europa’s surface releases particles that form a neutral gas envelope around the moon. Theoretical simulations (Johnson 1990;

Johnson et al. 2004; Shematovich et al. 2005; Smyth and Marconi 2006; Cassidy et al. 2007; 2010; Plainaki et al. 2010; 2012) predict that Europa's gas envelope consists mainly of three different populations (Fig. 5): (a) H₂O molecules, released through direct ion sputtering caused by the energetic ions of Jupiter's magnetosphere that impact the moon's surface; (b) O₂ and (c) H₂ molecules. The latter two species are produced through chemical reactions among different products of H₂O radiolytic decomposition. Sputtering also releases some minor surface species such as water group members (O, H, OH) and sodium or potassium (Brown and Hill 1996; Brown 2001; Leblanc et al. 2002, 2005; Cassidy et al. 2008 that populate the neutral gas envelope (for more details see Seki et al. 2015).

The presence of molecular oxygen in the exosphere of Europa has been proved only indirectly through either observations from the Earth or in situ measurements. The Goddard High-Resolution Spectrograph (GHRS) and the Advanced Camera for Surveys (ACS) on the Hubble Space Telescope (HST) observed the far-ultraviolet (UV) auroral emissions of atomic oxygen that were attributed to electron impact dissociative excitation of O₂ (Hall et al. 1995, 1998; Saur et al. 2011) with an estimated column density of $\sim 10^{14}$ to 10^{15} cm⁻². However, this column density estimate is quite uncertain since the Jovian magnetospheric electrons responsible for the observed emissions can be partially diverted and cooled through interactions with the atmosphere (Saur et al. 1998; Schilling et al. 2008). Kliore et al. (1997) estimated that the O₂ density (near the surface) required to produce the electron density observed by the Galileo spacecraft was $\sim 3 \times 10^{14}$ m⁻³. Observations acquired in 2001 by the Ultraviolet Imaging Spectrograph (UVIS) on the Cassini spacecraft during its flyby of Jupiter (Hansen et al. 2005) confirmed, independently, the presence of an O₂ atmosphere at Europa with a comparable column density to the one obtained through the ground-based observations. McGrath et al. (2004), based on the HST/Space Telescope Imaging Spectrograph (STIS) observations of Europa's trailing hemisphere, evidenced an asymmetric auroral emission at Europa, with a surplus in the anti-Jupiter direction with column density in the range $2\text{--}5 \times 10^{15}$ cm⁻². Saur et al. (2011) analyzed HST/ACS observations of Europa's leading hemisphere and estimated an O₂ column density lower by a factor 2–3 (1×10^{15} cm⁻²) than the one calculated by McGrath et al. (2004). Moreover, Saur et al. (2011) observed a surplus of emission at the apex of Europa's leading hemisphere. Roth (2012) suggested that some of these oxygen emissions may result from electron impact of water vapor plumes. Roth et al. (2014) claimed that the simultaneous observation of emissions from both atomic oxygen and atomic hydrogen were further evidence of the existence of water plumes erupting from the moon's surface.

Although H₂O is the dominant sputter product from water ice, O₂ is the dominant exospheric constituent because, unlike the water molecules, it does not freeze to the surface after being sputtered and returned to the surface by the moon's gravity (Johnson et al. 1982b; Shematovich et al. 2005; Luna et al. 2005). The oxygen molecules, unlike the other major water-dissociation product, H₂, also lack sufficient energy to overcome Europa's gravity (Smyth and Marconi 2006). As a result a thin and almost homogenous exospheric envelope (with thickness of some hundreds of kms), consisting of thermal O₂ molecules, with relatively high density, accumulates around the moon (Plainaki et al. 2012; 2013). At higher altitudes non-thermal exospheric O₂ dominates. On the basis of the Kliore et al. (1997) density values, Plainaki et al. (2010) estimated that the O₂ mean-free-path in Europa's atmosphere ranges from 13 km to 78 km. The scale-height estimations vary from 17 km to ~ 26 km (Ip 1996; Plainaki et al. 2010). Therefore, Europa's O₂ environment can be considered as a transitional case between a (collisional) atmosphere and a (collisionless) exosphere. Nonetheless this neutral environment is so tenuous that it does not act as a significant obstacle to escaping particles released from the moon surface. Tenuous as it is, the

neutral environment is still a barrier to magnetospheric bombardment: ionospheric conductivity results in the diversion of magnetospheric plasma flow around Europa (Saur et al. 1998). Europa's environment may work like a self-regulating system. The interaction may be self-limiting given that the ion bombardment with the surface creates the exosphere, but the exosphere (and ionosphere) limit ion bombardment by diverting plasma around Europa (Cassidy et al. 2013). The density of the overall oxygen exosphere is supplied until it reaches a steady state with exospheric loss processes (Johnson et al. 1982b, 1982a; Saur et al. 1998; Shematovich and Johnson 2001; Shematovich et al. 2005).

Saur et al. (1998) developed a 2D plasma model to study the interaction of the Jovian magnetosphere with the atmosphere/ionosphere of Europa and sources and sinks that maintain the neutral O₂ atmosphere. They concluded that the net mass balance between source and loss to/from the atmosphere is about $\sim 50 \text{ kg s}^{-1}$. The equivalent O₂ escape rate of $8.5 \times 10^{26} \text{ s}^{-1}$ is dominated by the loss of fast neutrals, produced mainly via ion sputtering, rather than the loss of ionospheric O²⁺ pickup ions. The calculated ionospheric density, generated by electron impact ionization, was $\sim 10^4 \text{ cm}^{-3}$, similar to measured values (Kliore et al. 1997). The Alfvénic current system closed by the ionospheric Hall and Pedersen conductivities carries a total current of $7 \times 10^5 \text{ A}$ in each Alfvén wing, which could contribute to the magnetic field disturbances observed by the Galileo spacecraft (Kivelson et al. 1997).

In contrast to O₂, the H₂ escape ratio is significantly higher and the hydrogen gas easily escapes from Europa's gravitational field (Plainaki et al. 2012). On the other hand, the H₂O escape rate is low because water molecules stick to the surface. The atmospheric density and residence time of H₂O in the exosphere are therefore considerably lower than those of O₂.

Different numerical, analytical and kinetic models have been developed to describe Europa's exosphere characteristics (Shematovich and Johnson 2001; Marconi 2003; Shematovich et al. 2005; Smyth and Marconi 2006; Plainaki et al. 2010, 2012, 2013). In particular, the Smyth and Marconi (2006) 2D axisymmetric kinetic model considered ion-neutral collisions in order to describe the physics in the lowest atmospheric layers above Europa's surface. Smyth and Marconi (2006) assumed that the source rates for the various species (H₂O, O₂, H₂ etc.) were determined by partitioning the O₂ source rate derived by the UV brightness of O emissions reported by Hall et al. (1995).

Recently, the Plainaki et al. (2012, 2013) 3D non-collisional Monte Carlo EGEON model described the main exospheric components that are directly generated by ion-sputtering and radiolysis. They found that the H₂O density due to ion sputtering is higher by a factor of ~ 6 on the trailing hemisphere, where the flux of Jupiter's energetic ions is higher on the leading hemisphere (Plainaki et al. 2012). Contrary to the H₂O case, the O₂ exospheric densities at high altitudes are higher on the sunlit hemisphere, thus having a periodic modulation during the moon's orbit around Jupiter (see Fig. 7 which illustrates the O₂ density spatial distribution due to magnetospheric ions impacting Europa). This happens because the temperature dependence (between 80 K at night and 130 K in the day-side) of yield values for O₂ release (Famà et al. 2008) is stronger than the effect of the enhanced trailing hemisphere bombardment. This model reproduces quite well the densities and illuminated/dark side asymmetries of the measured O₂ exosphere (Saur et al. 2011; McGrath et al. 2004). According to the EGEON model results, the observed surplus of OI emission at the 90° west longitude (leading hemisphere) (Saur et al. 2011) was due to the illumination of the leading hemisphere by the Sun that favors the radiolytic release of O₂ in the exosphere (Plainaki et al. 2013). Nevertheless, Cassidy et al. (2013) hypothesized that the yield, and therefore the actual release, has a delayed response to changes in temperature and therefore depends only on average ion precipitation. Although the Plainaki et al. (2013) model showed some global asymmetries in the O₂ density spatial distribution, it did

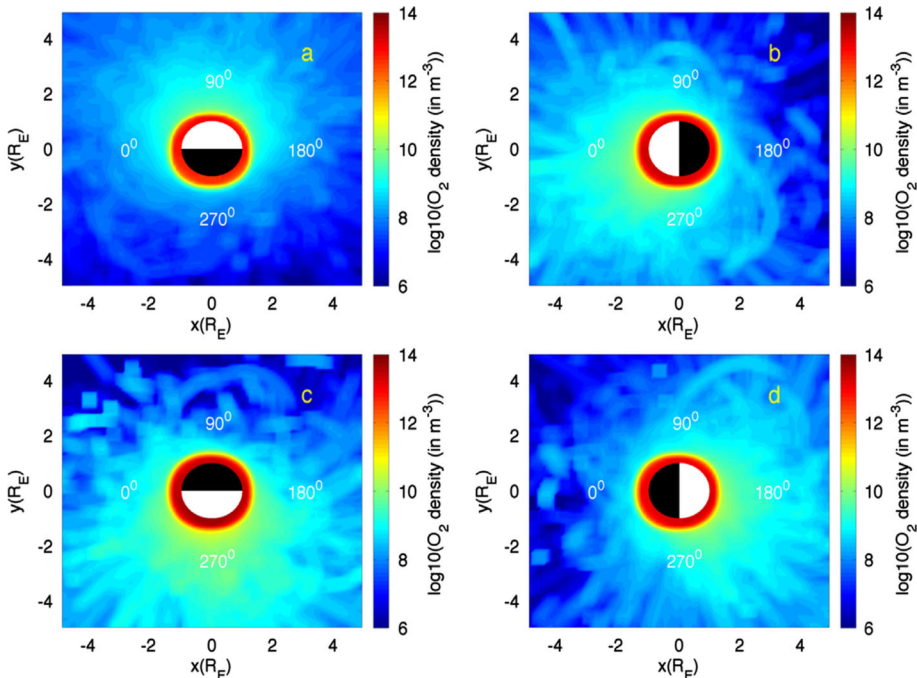


Fig. 7 Released O₂ density spatial distribution due to O⁺ magnetospheric ions impacting the surface of Europa obtained by EGEON for 4 configurations along the Europa's orbit around Jupiter. In all four panels the xy-plane is Europa's orbital plane around Jupiter. Sunlit hemisphere is indicated with white color and dark hemisphere with black. Jupiter is to the left and trailing hemisphere is down in all four configurations (Plainaki et al. 2013)

not reproduce any local asymmetries consistent with the surplus of atomic oxygen UV emission, observed on Europa's trailing hemisphere towards Jupiter (McGrath et al. 2004). There are three possible explanations of the enhanced emission: non-uniform surface composition (resulting in anisotropic release of surface material to the exosphere); local surface activity (suggested by the recent water plume observation of Roth et al. 2014); and/or spatial variation of the impacting electron flux.

The material escaping from Europa's atmosphere is distributed along Europa's orbit forming an extensive neutral cloud. Charge exchange of inwardly-diffusing energetic ions with these neutrals generates energetic neutral atoms that were observed by the Cassini/INCA instrument (Mauk et al. 2003). The two most important escaping water group species are H₂ and O (Smyth and Marconi 2006), that are highly peaked about the satellite location and hence highly asymmetrically distributed around Jupiter, and have substantial forward clouds that extend radially inward to Io's orbit (Fig. 5). The H₂ and O neutral clouds provide a new source of molecular and atomic pickup ions for the thermal plasma; furthermore, the cooler iogenic plasma is transported radially outwards distributing from Io to Europa orbit. Smyth and Marconi (2006) estimated the spatially integrated instantaneous ion mass-loading rate for the H₂ cloud to be $\sim 9.3 \text{ kg s}^{-1}$ for the H₂ cloud and $\sim 10.6 \text{ kg s}^{-1}$ for the O cloud from electron impact and charge exchange processes. Estimates of ionization of the O cloud range from $4.4 \times 10^{25} \text{ O/s}$ (Nagy et al. 1998) and $6.5 \times 10^{25} \text{ O/s}$ (2 kg/s) (Plainaki et al. 2013) to $2.6 \times 10^{26} \text{ O/s}$ ($\sim 5\text{--}10 \text{ kg s}^{-1}$) (Shematovich et al. 2005;

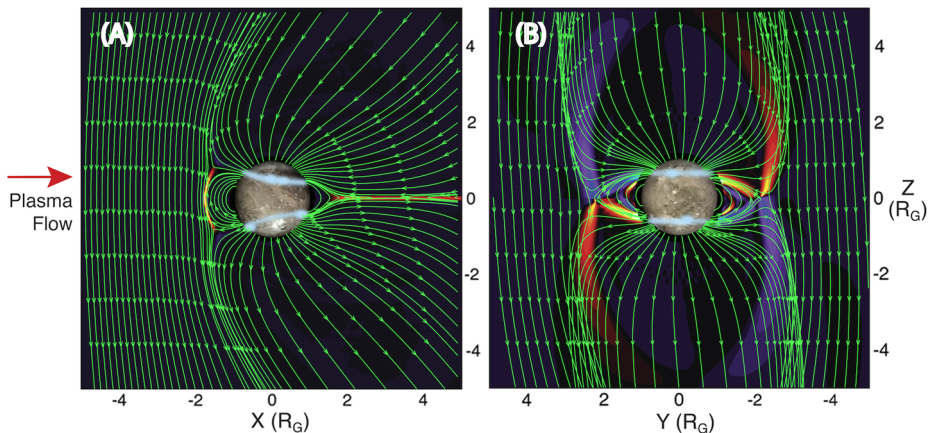


Fig. 8 Numerical model of the magnetosphere of Ganymede, with the satellite and the location of the auroral emissions superimposed (based on Jia et al. 2008). (A) The view looking at the anti-Jupiter side of Ganymede. (B) The view looking in the direction of the plasma flow at the upstream side (orbital trailing side) of Ganymede, with Jupiter to the left. *The shaded areas show the regions of currents parallel to the magnetic field*

Smyth and Marconi 2006). Plainaki et al. (2013) suggest that the O supply rate is modulated along Europa's orbit, being larger by a factor up to 4 when the trailing side is illuminated.

6 Ganymede

Jupiter's Galilean satellite Ganymede, with a radius of ~ 2634 km, is the largest moon in the solar system. It was discovered during the Galileo mission that Ganymede possesses an intrinsic magnetic field (Kivelson et al. 1996). The interaction between Jupiter's magnetospheric plasma and Ganymede's intrinsic magnetic field, whose equatorial surface field strength is about 7 times the background Jovian field, results in a mini-magnetosphere surrounding the moon (Fig. 8). Ganymede's magnetosphere is unique in that it is so far the only known satellite with an intrinsic field forming its own magnetosphere within a planetary magnetosphere (Jia et al. 2010a). The moon's magnetosphere has exhibited a variety of previously unknown phenomena revealed by the Galileo mission, including well-defined magnetospheric boundaries and magnetic perturbations associated with the intrinsic field (Kivelson et al. 1998), a rich subset of wave modes like those found within any planetary magnetosphere (Gurnett et al. 1996; Kurth et al. 1997), a significant population of charged particles associated with the moon (Frank et al. 1997a; Williams et al. 1997) and the existence of polar aurorae emitted from the atmosphere (Feldman et al. 2000; McGrath et al. 2013) shown in Fig. 9. Ganymede auroral emission has different morphologies dependent on the hemisphere of the moon and the interaction with the magnetospheric plasma.

At Ganymede's orbit, the corotating plasma of Jupiter's magnetosphere typically flows relative to the moon at speeds smaller than the ambient Alfvén speed. As a consequence, there is no bow shock formed in front of the magnetosphere. Instead, the incident Jovian plasma is slowed down by the interaction with magnetosonic waves that propagate upstream. The sub-Alfvénic interaction results in a magnetospheric configuration at

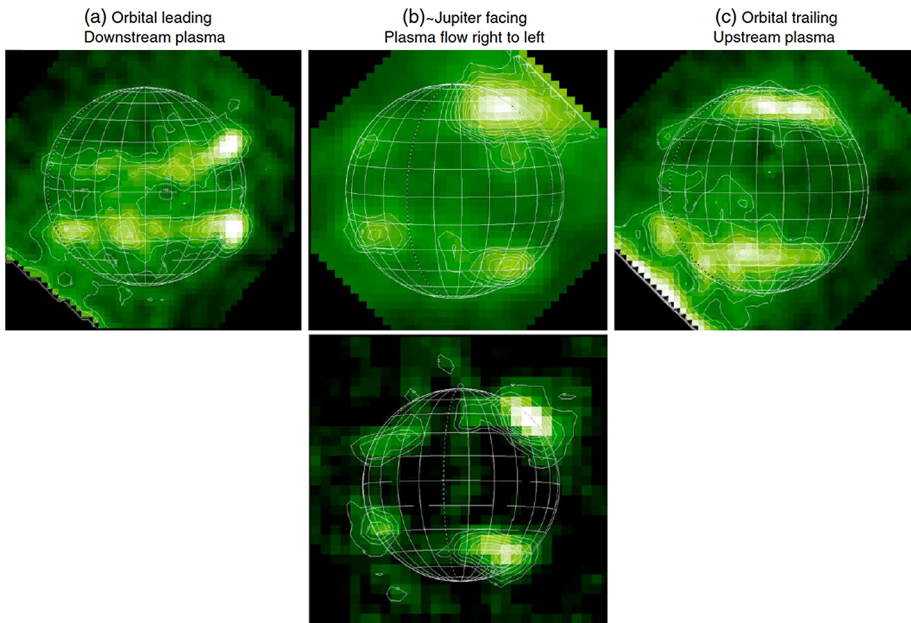


Fig. 9 Ganymede auroral emission from atomic oxygen illustrating the different morphologies on the different hemispheres of the satellite. The magnetospheric plasma flow is into the page for the trailing hemisphere, out of the page for the leading hemisphere, and approximately from right to left for the Jupiter-facing hemisphere (from McGrath et al. 2013)

Ganymede rather different from that of planetary magnetospheres arising from interactions with the super-Alfvénic and supersonic solar wind (except on extremely rare occasions when the solar wind is sub-Alfvénic, see Chané et al. 2012). A pair of the so-called Alfvén wings (Neubauer 1980, 1998; Southwood et al. 1980) form that extend almost vertically in the north-south direction, leading to a cylindrical shape of the magnetosphere in contrast to the bullet shape of planetary magnetospheres (see Fig. 8, Jia et al. 2008). While some of the incident flow diverts around the magnetosphere and is accelerated on the flanks (Frank et al. 1997a), the ambient plasma appears to gain significant access into the magnetosphere through magnetic reconnection, because Ganymede's intrinsic field is nearly anti-parallel to the external field near the equator at all times (Kivelson et al. 1998; Jia et al. 2010b). Plasma enters the Alfvén wings via magnetopause reconnection and is then convected across the polar caps towards the downstream region. Within the Alfvén wings, the plasma flow is significantly decelerated (Frank et al. 1997a; Williams et al. 1998) and the disturbances associated with the deceleration propagate away from the moon along the magnetic field lines via Alfvén waves that carry field-aligned currents. As with Io and Europa, the presence of field-aligned currents linking Ganymede to Jupiter's ionosphere has been confirmed by the discovery of ultraviolet emissions at the foot of Ganymede's flux tube in Jupiter's auroral images (Clarke et al. 2002; Grodent et al. 2009). Reconnection is expected to occur in Ganymede's magnetotail that eventually returns part of the flow back towards the moon and the upstream magnetosphere, and ejects the rest down the tail.

The plasma entering inside Ganymede's magnetosphere and impacting onto the surface, as in the Europa case, causes particle release generating a tenuous atmosphere/thick ex-

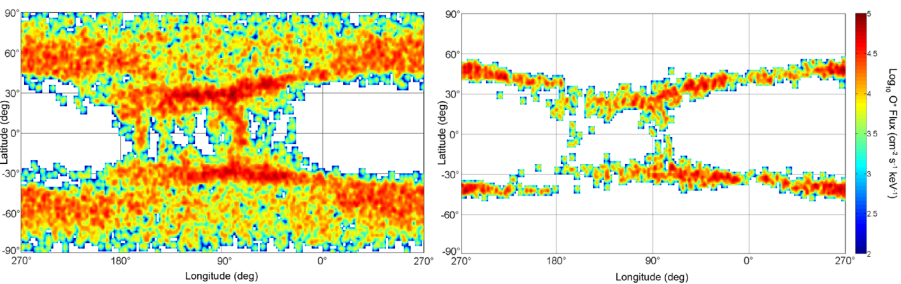


Fig. 10 Plainaki-1: Precipitation map of the O^+ differential flux ($\text{cm}^{-2} \text{s}^{-1} \text{sr}^{-1} \text{keV}^{-1}$) around Ganymede at initial energy equal to 10 keV in the hypothesis of full mirroring in the Jupiter's magnetosphere (*left*) and non-mirroring (*right*) assumption. Jupiter is at 0° longitude, leading at 90° . The colorbar scale is logarithmic

osphere. In fact, Jupiter's magnetospheric ions precipitating onto the surface cause sputtering, ionization and excitation of water-ice molecules, followed partially by dissociation; chemical reactions among the water-dissociation products result in the formation of new molecules (e.g. O_2 , H_2 , OH and minor species) that are finally ejected from the surface into Ganymede's exosphere. H_2 formed in ice diffuses and escapes much more efficiently than O_2 at the relevant temperatures in the outer solar system; moreover, H_2 escapes from the icy moons because of its low mass and the relatively weak gravitational fields. Therefore, the irradiation of Ganymede's surface can preferentially populate the magnetosphere with hydrogen, as is the case at Europa (Lagg et al. 2003; Mauk et al. 2003), leaving behind an oxygen-rich satellite surface (Johnson et al. 2004).

While the precipitation onto the surface is a loss process for Jupiter's magnetosphere, the ionization of the released exospheric particles provides a new source for Ganymede's ionosphere. These newly formed ions, after a chain of processes, could become again magnetospheric ions in Jupiter's magnetosphere.

Plainaki et al. (2015) showed that the plasma precipitation at Ganymede occurs in a region related to the Open/Closed magnetic Field line Boundary (OCFB) location, that is in good agreement with the Galileo magnetic field and plasma flow measurements (Gurnett et al. 1996; Kivelson et al. 1996, 1998). As shown in Fig. 10, the extent of the plasma precipitation regions depends on the assumption used to mimic the plasma mirroring in Jupiter's magnetosphere. In particular, in the hypothesis of efficient mirroring in Jupiter's magnetosphere, the O^+ precipitation takes place if the ions are assumed precipitating over the whole polar cap. If no mirroring is considered, the O^+ precipitation is confined to a latitudinal zone that is $\sim 10^\circ$ wide and centered at the OCFB (i.e., at a latitude of $\sim 50^\circ$ in the North trailing hemisphere). Moreover, in the latter case, the total rate of precipitating ions is lower (see Fig. 10). Nevertheless, the real ion-mirroring rate is expected to have an intermediate value between 0 and 100 %, since the ion population is confined inside the Jupiter Plasma Sheet (being partially reflected and partially lost). The sputtered H_2O density distribution mimics the morphology of the plasma impact to the surface as predicted by the global MHD model of Ganymede's magnetosphere (Jia et al. 2009) for the case that the moon is located close to the center of Jupiter plasma sheet. Indeed, both in the northern and southern hemispheres the sputtered H_2O exospheric density maximum is located at higher latitudes in the trailing hemisphere than in the leading one. Moreover, in the full mirroring assumption, the primary surface sputtering mechanism at the whole polar cap of Ganymede can alone explain the observed higher albedo of this region (Khurana et al. 2007); in the non-mirroring assumption the polar cap brightness above the OCFB ring can

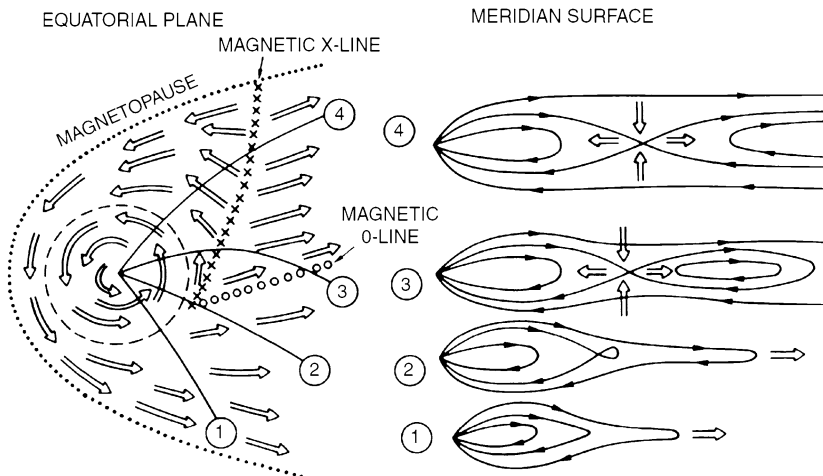


Fig. 11 Sketch of the global flow patterns of the Jovian magnetosphere known as the Vasyliunas-cycle (from Vasyliunas 1983)

be explained with the action of secondary sputtering due to ionized exospheric particles re-impacting the surface. A sublimated H₂O population adds to this sputtered population close to the subsolar point. Finally the estimated total surface release rate of sputtered H₂O molecules is $7 \times 10^{25} \text{ s}^{-1}$ whereas the release rate of the sublimated H₂O is $7 \cdot 10^{29} \text{ s}^{-1}$. The plasma effects on the exosphere generation are less evident in the O₂ density distribution, since this molecule does not stick onto the surface and thermalizes. Indeed, the energetic O₂ emission has a distribution that depends both on the morphology of the plasma precipitation to the surface and on the Sun illumination that determines the efficiency of the radiolysis mechanism, on the illuminated side (Plainaki et al. 2015).

The rates of the most important plasma-moon interactions leading to the loss of Ganymede's exosphere (and to a source for the magnetosphere) were calculated by Plainaki et al. (2015), who used previously published estimates of the plasma parameters (Kivelson et al. 2004; McNutt et al. 1981; Scudder et al. 1981; Gurnett et al. 1996; Eviatar et al. 2001) of the ambient magnetospheric environment at Ganymede, together with laboratory-based estimates of rate coefficients (for a review see Burger et al. 2010). They showed that the loss rate for H₂O in the polar caps is due to its charge exchange with ionospheric O₂⁺ and is of the order of 10^{-5} s^{-1} ; in the closed field lines region, the H₂O loss rate is of the order of 10^{-6} s^{-1} and is mainly due to charge exchange between ionospheric O⁺ and H₂O. The exospheric O₂ net loss rate in the polar caps is due to electron impact ionization and is in the range 9×10^{-8} – $9 \times 10^{-7} \text{ s}^{-1}$ (the minimum value is where the electron density is lower, likely where the neutral density is higher); on the illuminated side the O₂ loss rate is of the order of $\sim 10^{-7} \text{ s}^{-1}$ whereas on the night side of the closed field lines region it is of the order of 10^{-8} s^{-1} .

Ions outflowing from Ganymede's ionosphere across the polar cap were detected during Galileo's polar flyby (Frank et al. 1997b). The ionospheric outflows were originally identified as hydrogen ions (Frank et al. 1997b; Paty et al. 2008) and later reinterpreted as atomic oxygen ions (Vasyliunas and Eviatar 2000; Jia et al. 2009). In either case, it is suggested that there appears to be a polar wind similar to that observed in the terrestrial magnetosphere. Using Galileo's Plasma Spectrometer (PLS) measurements and assuming a circular area with radius of 1 Ganymede radius for the outflow region, Frank et al. (1997b) estimated the total

ionospheric outflow rate to be $\sim 6 \times 10^{25}$ ions/s. While the fate of the ionospheric outflows is poorly known due to lack of observations, it is likely that some of the outflowing plasma will participate in the tail reconnection, through which a fraction of the ionospheric plasma will be recycled back into Ganymede's magnetosphere and the rest will be released down the tail to the ambient environment, providing a plasma source for Jupiter's magnetosphere albeit with a supply rate much smaller than from the moon Io.

In addition to the ionospheric outflows, the pickup of neutral particles originating from Ganymede's atmosphere (Hall et al. 1998) may also provide a plasma source to Jupiter's magnetosphere. Volwerk et al. (2013) recently analyzed the Galileo magnetometer measurements acquired during two upstream flybys, and found signatures of ion cyclotron waves near water-group ion gyro frequencies outside of the magnetosphere, which are indicative of pick-up of newly ionized particles from the moon's extended exosphere. Nonetheless, the estimated pickup rate of $\sim 5 \times 10^{23}$ ions s $^{-1}$ is several orders of magnitude smaller than the ionospheric outflow rate, making the pickup ions from Ganymede's atmosphere a rather minor source of plasma for Jupiter's magnetosphere.

7 Solar Wind

There is evidence that the solar wind is a source of plasma to Jupiter's magnetosphere via magnetic reconnection, although the precise role of the solar wind in terms of driving a Dungey cycle at Jupiter is unclear. Other transport processes such as the Kelvin-Helmholtz instability can also be at work (e.g. Delamere and Bagenal 2010; Ma et al. 2014a, 2014b). The ion composition of the boundary layers, inside of the magnetopause, is consistent with mass transport at the magnetopause. At Jupiter Bame et al. (1992) reported ion composition in the boundary layer during the expansion of the magnetopause past the Ulysses spacecraft. The magnetopause was not a sharp spatial boundary, and rather magnetosheath and magnetospheric populations were observed to coexist within the boundary layer internal to the magnetopause. A boundary layer was clearly present for all but one of the Jovian magnetopause crossings. Similarly, Galvin et al. (1993) and Phillips et al. (1993) reported a mixed boundary layer composition and Galvin et al. (1993) suggested that transport across the magnetopause boundary can work both ways. A significant finding by Hamilton et al. (1981) from the Voyager 2 Low Energy Charged Particle instrument (LECP) data is that the plasma sheet composition beyond 60–80R_J in the tail is similar to that of solar wind energetic ions while the inner magnetosphere is dominated by iogenic material. Krupp et al. (2004a) discussed evidence of a boundary layer seen in the Cassini Magnetosphere Imaging Instrument/Low Energy Magnetospheric Measurement System (MIMI/LEMMS) energetic electron data when Cassini skimmed Jupiter's dusk magnetopause during the gravity assist flyby. They suggest that the leakage of energetic magnetospheric electrons to the magnetosheath is consistent with open field lines planetward of the magnetopause. Most recently, the particles measured by New Horizons as it traversed down the flanks of the magnetotail were increasingly dominated by light ions at farther distances down-tail (Haggerty et al. 2009; Hill et al. 2009; Ebert et al. 2010).

Hill et al. (1983) estimated the solar wind source by taking the fraction of solar wind leaking into the magnetosphere to be $\sim 10^{-3}$ and obtained a tiny source strength of 20 kg s $^{-1}$ for a radius of cross-section of 100R_J. Bagenal and Delamere (2011) took a more realistic cross-section of the terminator of 150R_J, a local solar wind density of 1 cm $^{-3}$ and speed of 400 km/s and estimated a solar wind flux of ~ 230 tons s $^{-1}$, which makes a source of

230 kg s^{-1} for the Hill et al. (1983) 0.1 % leakage rate. Even with such low mass source rates, the enhanced density of protons will significantly alter the ion composition of the outer boundary layers.

8 Other Sources

At Saturn, the rings provide an important source of plasma for the magnetosphere. Although no such information is currently available regarding Jupiter, using the Saturn analogy the rings are also likely to be a source at Jupiter. The lack of relevant data so far probably implies that this source is small or negligible.

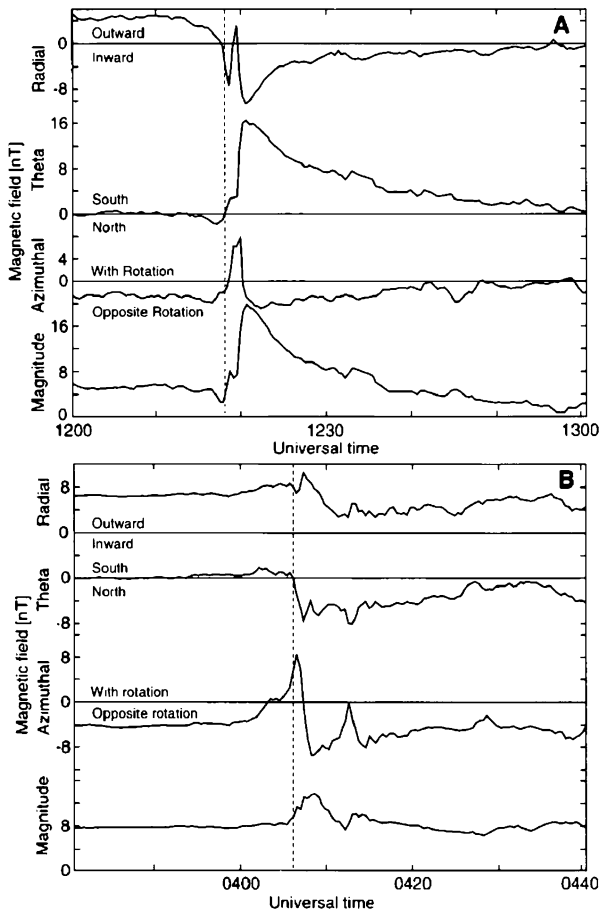
9 Transport Mechanisms

Jupiter is a rapidly rotating planet with the volcanic moon Io acting as a strong internal plasma source. In this case, the driving of magnetospheric dynamics by the (external) solar wind is thought to be secondary to the role of the (internally-driven) rotation (Hill et al. 1974; Michel and Sturrock 1974; Vasylunas 1983; Kivelson and Southwood 2005). In what has become known as the Vasylunas cycle shown in Fig. 11, the plasma created deep within the rapidly-rotating magnetosphere is accelerated by magnetic stresses from the ionosphere, gains energy, and moves outward from the planet. Centrifugal forces cause the field lines to stretch. These stretched field lines can form a thin current sheet, across which the closed field lines reconnect. This reconnection simultaneously shortens the field line and can release plasma down the tail in the form of a “plasmoid”.

In order to observe the passage of plasmoids over the spacecraft, one should examine the north-south component of the magnetic field, to look for deflections from the radially stretched configuration. The Voyager flyby data gave a hint of reconnection processes in the Jovian tail (Nishida 1983), but it was only with the arrival of the Galileo orbiter in 1995 that the properties of reconnection at Jupiter could be probed in detail. One of the first studies to employ Galileo data to show evidence of plasmoid break-off was by Russell et al. (1998), and Fig. 12 shows an example of two characteristic magnetic field signatures. The sign of the change in the north-south component of the field provides information as to which side of the reconnection x -line the spacecraft is on and in this case the two events shown in Fig. 12 were on opposite sides of the x -line. In addition to magnetometer data, Galileo energetic particle detector data have been used to reveal evidence for both tailward and planetward plasma flows associated with magnetic reconnection, and thus to infer the position of the x -line in Jupiter’s tail (Woch et al. 2002; Kronberg et al. 2008). The most comprehensive study to date was performed by Vogt et al. (2010), who surveyed all available Galileo data and identified 249 reconnection events, the locations of which are shown in Fig. 13. From this they extracted a statistical x -line extending from $\sim 90R_J$ at dawn to $\sim 120R_J$ downtail at dusk.

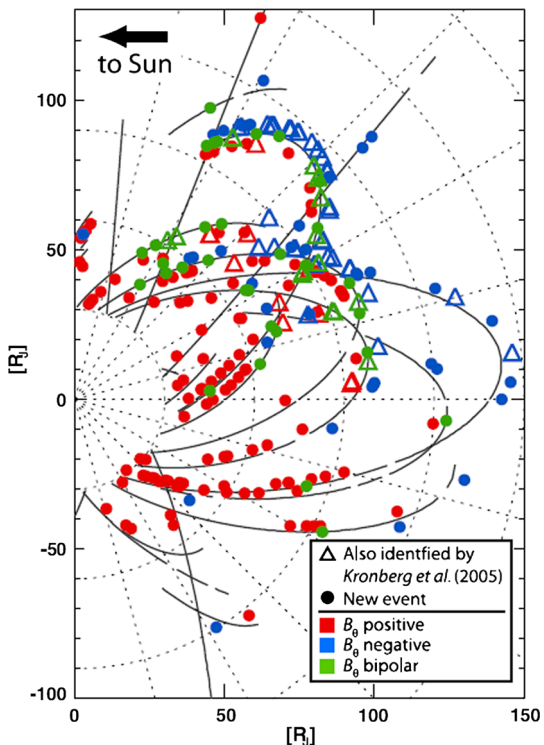
In order to estimate the effect of reconnection as a mechanism to remove mass from the magnetosphere, one must first obtain estimates of the size and composition of plasmoids. Kronberg et al. (2008) presented statistics on the length of Jovian plasmoids, based on measurements taken using the Galileo energetic particles detector. They found a typical length of $\sim 9R_J$. In order to translate size estimates into mass calculations, Bagenal (2007) assumed that a typical plasmoid is a disk with a $25R_J$ diameter and $10R_J$ height, with density 0.01 cm^{-3} , and calculated that releasing one plasmoid per day (higher than the observed

Fig. 12 Two events which display north-south and south-north turnings of the magnetic field in Jupiter's tail, indicative of the presence of reconnection event(s) planetward/tailward of the spacecraft (from Russell et al. 1998)



2–3 day recurrence period) is equivalent to a mass loss rate of only ~ 30 kg/s. More recently, a survey of 43 plasmoids identified with the Galileo magnetometer found a mean length of $\sim 3R_J$ and a mass loss rate ranging from 0.7–120 kg/s (Vogt et al. 2014). It is clear that reconnection is active at Jupiter, and New Horizons data from deep in the Jovian tail confirm that iogenic material that has perhaps been broken off by reconnection is present many hundreds of R_J from the planet (Haggerty et al. 2009). However, regardless of the range of assumptions made, all studies indicate that the estimated rate of mass release supported by the observed plasmoids at Jupiter is far lower than the rate of plasma input from Io (260–1400 kg/s). Thus this has led authors such as Bagenal and Delamere (2011) to consider alternative mass loss pathways such as diffusive processes, or small-scale “drizzle” down the tail or loss across the magnetopause via small-scale intermittent reconnection. Although plasmoid ejection seems to play a relatively minor role in mass transport at Jupiter (hence opening up the possibility of important diffusive processes), it appears that tail reconnection is an important method of magnetic flux transport. For example, analysis of the observed plasmoids at Jupiter suggests an average flux closure rate of ~ 7 –70 GWb/day (Vogt et al. 2014), which closely matches the estimated rate of average flux opening through dayside reconnection, 18 GWb/day (Nichols et al. 2006).

Fig. 13 Location of 249 reconnection events identified using the Galileo magnetometer (from Vogt et al. 2010)



10 Summary

The giant magnetosphere of Jupiter is fuelled primarily by the ionization of volcanic gases from Io, with additional minor sources from the other, icy, Galilean moons. There is likely a source of light ions from the atmosphere and ionosphere of Jupiter but it has neither been accurately measured nor modelled. The polar passes of the Juno mission will hopefully shed light on this possible contribution from the planet. While the radial transport mechanism in the plasma disc is described as flux tube interchange diffusion, the controlling factors, however, are not well quantified. Two major mysteries at Jupiter are the mechanism that heats the plasma as it moves outwards from the Io plasma torus, and the mechanism by which plasma is lost from the system. Some outstanding questions are as follows:

- What are the timescales for variability of the production of plasma at Io, as well as the other Galilean moons?
- What are the amounts of plasma that enter the Jovian plasma sheet from the atmosphere and ionosphere of Jupiter and from the solar wind? On what do these source rates depend?
- How do the plasma sheet properties (density, temperature, radial transport) respond to variability in the plasma sources?
- How is the main auroral emission affected by changes in the iogenic plasma production rate?

It is hoped that exploration of the Jovian system by NASA's Juno mission (2016–2018) and ESA's JUpiter ICy moons Explorer (JUICE) mission will answer these questions.

Acknowledgements The work of X. Jia was supported by the NASA Outer Planets Research Program through grant NNX12AM74G. The work of M. Blanc was done thanks to support by IRAP (CNRS and University of Toulouse). The work of F. Bagenal was funded by NASA JDAP program (grant number NNX09AE03G). C.M. Jackman was funded by a Science and Technology Facilities Council Ernest Rutherford Fellowship. The work by A. Kotova was financed by the International Max Planck Research School on Physical processes in the Solar System and Beyond (IMPRS) at the Max Planck Institute for Solar System Research (MPS). Work by N. Krupp at MPS was in part financed by the German BMWi through the German Space Agency DLR under contracts 50 OH 0301, 50 OH 0801, 50 OH 0802, 50 OH 1101, 50 OH 1502, 50 ON 0201, 50 QJ 1301, 50 OO 1206, 50 OO 1002 and by the Max Planck Society. This work was also supported by the European Research Infrastructure EUROPLANET RI in the framework program FP7, contract number: 001637. Work by T. Cassidy was NASA OPR Grant NNX13AE65G (through JPL subcontract 1440362). Work by E. Chané was funded by the Interuniversity Attraction Poles Programme of the Belgian Science Policy Office (IAP P7/08 CHARM) and by the Research Foundation-Flanders (FWO 12M0115N).

Conflict of interest The authors declare that they have no conflict of interest.

References

- I.I. Alexeev, E.S. Belenkaya, Modeling of the Jovian magnetosphere. *Ann. Geophys.* **23**, 809–826 (2005)
- F. Bagenal, The magnetosphere of Jupiter: Coupling the equator to the poles. *J. Atmos. Sol.-Terr. Phys.* **69** (2007)
- F. Bagenal, P.A. Delamere, Flow of mass and energy in the magnetospheres of Jupiter and Saturn. *J. Geophys. Res.* **116**, A05209 (2011). doi:[10.1029/2010JA016294](https://doi.org/10.1029/2010JA016294)
- F. Bagenal, T. Dowling, W. McKinnon (eds.), *Jupiter: Planet, Satellites, Magnetosphere* (Cambridge University Press, Cambridge, 2004)
- F. Bagenal, A. Adriani, F. Allegrini, S.J. Bolton, B. Bonfond, E.J. Bunce, J.E.P. Connerney, S.W.H. Cowley, R.W. Ebert, G.R. Gladstone, C.J. Hansen, W.S. Kurth, S.M. Levin, B.H. Mauk, D.J. McComas, C.P. Paranicas, D. Santos-Costa, R.M. Thorne, P. Valek, J.H. Waite, P. Zarka, Magnetospheric science objectives of the Juno mission. *Space Sci. Rev.* (2014). doi:[10.1007/s11214-014-0036-8](https://doi.org/10.1007/s11214-014-0036-8)
- S.J. Bame, B.L. Barraclough, W.C. Feldman, G.R. Gisler, J.T. Gosling, D.J. McComas, J.L. Phillips, M.F. Thomsen, B.E. Goldstein, M. Neugebauer, Jupiter's magnetosphere: Plasma description from the Ulysses flyby. *Science* **257**, 1539–1543 (1992)
- S.J. Bolton, The Juno mission, in *Proceedings of the International Astronomical Union, IAU Symposium*, vol. 269 (2010), pp. 92–100
- S. Bolton, R. Thorne, S. Bourdarie, I. DePater, B. Mauk, Jupiter's inner radiation belts, in *Jupiter: Planet, Satellites, Magnetosphere*, ed. by F. Bagenal, T.E. Dowling, W.B. McKinnon (Cambridge University Press, Cambridge, 2004)
- B. Bonfond, D. Grodent, J.-C. Gérard, T. Stallard, J.T. Clarke, M. Yoneda, A. Radioti, J. Gustin, Auroral evidence of Io's control over the magnetosphere of Jupiter. *Geophys. Res. Lett.* **39**, L01105 (2012). doi:[10.1029/2011GL050253](https://doi.org/10.1029/2011GL050253)
- S.J. Bolton et al., The Juno mission, *Space Sci. Rev.* (2015, submitted)
- S.W. Bouger et al., Jupiter's general circulation model (JTGCM): Global structure and dynamics driven by auroral and Joule heating. *J. Geophys. Res.* **110**, E04008 (2005). doi:[10.1029/2003JE002230](https://doi.org/10.1029/2003JE002230)
- M.E. Brown, Potassium in Europa's atmosphere. *Icarus* **151**, 190–195 (2001)
- M.E. Brown, R.E. Hill, Discovery of an extended sodium atmosphere around Europa. *Nature* **380**, 229–231 (1996)
- M.H. Burger, R. Wagner, R. Jaumann, T.A. Cassidy, Effects of the external environment on icy satellites. *Space Sci. Rev.* **153**(1–4), 349–374 (2010)
- T.A. Cassidy, R.E. Johnson, M.A. McGrath, M.C. Wong, J.F. Cooper, The spatial morphology of Europa's near-surface O₂ atmosphere. *Icarus* **191**, 755–764 (2007)
- T.A. Cassidy, R.E. Johnson, P.E. Geissler, F. Leblanc, Simulation of Na D emission near Europa during eclipse. *J. Geophys. Res.* **113**, E02005 (2008)
- T. Cassidy, P. Coll, F. Raulin, R.W. Carlson, R.E. Johnson, M.J. Loeffler, K.P. Hand, R.A. Baragiola, Radiolysis and photolysis of icy satellite surfaces: Experiments and theory. *Space Sci. Rev.* **153**(1–4), 299–315 (2010)
- T.A. Cassidy, C.P. Paranicas, J.H. Shirley, J.B. Dalton III., B.D. Teolis, R.E. Johnson, L. Kamp, A.R. Hendrix, Magnetospheric ion sputtering and water ice grain size at Europa. *Planet. Space Sci.* **77**, 64–73 (2013)
- G. Caudal, A self-consistent model of Jupiter's magnetodisc including the effects of centrifugal force and pressure. *J. Geophys. Res.* **91**, 4201–4221 (1986). doi:[10.1029/JA091iA04p04201](https://doi.org/10.1029/JA091iA04p04201)

- E. Chané, J. Saur, F.M. Neubauer, J. Raeder, S. Poedts, Observational evidence of Alfvén wings at the Earth. *J. Geophys. Res. Space Phys.* **117**, A09217 (2012). doi:[10.1029/2012JA017628](https://doi.org/10.1029/2012JA017628)
- E. Chané, J. Saur, S. Poedts, Modeling Jupiter's magnetosphere: Influence of the internal sources. *J. Geophys. Res. Space Phys.* **118**, 2157–2172 (2013). doi:[10.1002/jgra.50258](https://doi.org/10.1002/jgra.50258)
- S. Chapman, V.C.A. Ferraro, A new theory of magnetic storms. *Nature* **126**, 129–130 (1930)
- C.F. Chyba, Energy for microbial life on Europa. *Nature* **403**, 381–382 (2000)
- J.T. Clarke, J. Ajello, G. Ballester, L.B. Jaffel, J. Connerney, J.C. Gerard, G.R. Gladstone, D. Grodent, W. Pryorl, J. Trauger, J.H.W. Jr, Ultraviolet emissions from the magnetic footprints of Io, Ganymede and Europa on Jupiter. *Nature* **415**, 997–1000 (2002)
- J. Clarke, D. Grodent, S. Cowley, E. Bunce, P. Zarka, J. Connerney, T. Satoh, Jupiter's aurora, in *Jupiter: Planet, Satellites, Magnetosphere*, ed. by F. Bagenal, T.E. Dowling, W.B. McKinnon (Cambridge University Press, Cambridge, 2004)
- J.E.P. Connerney, M.H. Acuna, N.F. Ness, Modeling the Jovian current sheet and inner magnetosphere. *J. Geophys. Res.* **86**, 8370–8384 (1981). doi:[10.1029/JA086iA10p08370](https://doi.org/10.1029/JA086iA10p08370)
- J.F. Cooper, R.E. Johnson, B.H. Mauk, H.B. Garrett, N. Gehrels, Energetic ion and electron irradiation of the icy Galilean Satellites. *Icarus* **149**, 133–159 (2001)
- S.W.H. Cowley, E.J. Bunce, Origin of the main auroral oval in Jupiter's coupled magnetosphere-ionosphere system. *Planet. Space Sci.* **49**, 1067–1088 (2001)
- T.E. Cravens, vibrationally excited molecular hydrogen in the upper atmosphere of Jupiter. *J. Geophys. Res.* **92**, 11083 (1987)
- P.A. Delamere, F. Bagenal, Solar wind interaction with Jupiter's magnetosphere. *J. Geophys. Res.* **115**(A), A10201 (2010). doi:[10.1029/2010JA015347](https://doi.org/10.1029/2010JA015347)
- A. Dessler (ed.), *Physics of the Jovian Magnetosphere* (Cambridge University Press, Cambridge, 1983)
- R.W. Ebert, D.J. McComas, F. Bagenal, H.A. Elliott, Location, structure, and motion of Jupiter's dusk magnetospheric boundary from 1625 to 2550 RJ. *J. Geophys. Res.* **115**, 12,223 (2010)
- R.W. Ebert, F. Bagenal, D.J. McComas, C.M. Fowler, A survey of solar wind conditions at 5 AU: A tool for interpreting solar wind-magnetosphere interaction at Jupiter. *Front. Astron. Space Sci.* **1**, 4 (2014). doi:[10.3389/fspas.2014.00004](https://doi.org/10.3389/fspas.2014.00004)
- T.M. Edwards, E.J. Bunce, S.W.H. Cowley, A note on the vector potential of Connerney et al.'s model of the equatorial current sheet in Jupiter's magnetosphere. *Planet. Space Sci.* **49**, 1115–1123 (2001). doi:[10.1016/S0032-0633\(00\)00164-1](https://doi.org/10.1016/S0032-0633(00)00164-1)
- R.E. Ergun, L. Ray, P.A. Delamere, F. Bagenal, V. Dols, Y.-J. Su, Generation of parallel electric fields in the Jupiter-Io torus wake region. *J. Geophys. Res.* **114**, 5201 (2009)
- A. Aviatar, V.M. Vasylunas, D.A. Gurnett, The ionosphere of Ganymede. *Planet. Space Sci.* **49**, 327–336 (2001). doi:[10.1016/S0032-0633\(00\)00154-9](https://doi.org/10.1016/S0032-0633(00)00154-9)
- M. Famà, J. Shi, R.A. Baragiola, Sputtering of ice by low-energy ions. *Surf. Sci.* **602**, 156–161 (2008)
- P.D. Feldman, M.A. McGrath, D.F. Strobel, H.W. Moos, K.D. Retherford, B.C. Wolven, HST/STIS ultraviolet imaging of polar aurora on Ganymede. *Astrophys. J.* **535**, 1085–1090 (2000)
- L.A. Frank, W.R. Paterson, K.L. Ackerson, S.J. Bolton, Low-energy electrons measurements at Ganymede with the Galileo spacecraft: Probes of the magnetic topology. *Geophys. Res. Lett.* **24**(17), 2,159–2,162 (1997a)
- L.A. Frank, W.R. Paterson, K.L. Ackerson, S.J. Bolton, Outflow of hydrogen ions from Ganymede. *Geophys. Res. Lett.* **24**(17), 2151–2154 (1997b)
- K. Fukazawa, T. Ogino, R.J. Walker, Dynamics of the Jovian magnetosphere for northward interplanetary magnetic field (IMF). *Geophys. Res. Lett.* **32**, L03,202 (2005). doi:[10.1029/2004GL021392](https://doi.org/10.1029/2004GL021392)
- A.B. Galvin, C.M.S. Cohen, F.M. Ipavich, R. von Steiger, J. Woch, U. Mall, Boundary layer ion composition at Jupiter during the inbound pass of the Ulysses flyby. *Planet. Space Sci.* **41**, 869–876 (1993)
- O. Grasset et al., JUpiter ICy moons Explorer (JUICE): An ESA mission to orbit Ganymede and to characterise the Jupiter system. *Planet. Space Sci.* **78**, 1–21 (2013)
- D. Grodent, B. Bonfond, A. Radioti, J.-C. Gérard, X. Jia, J.D. Nichols, J.T. Clarke, Auroral footprint of Ganymede. *J. Geophys. Res.* **114**(A7) (2009). doi:[10.1029/2009JA014289](https://doi.org/10.1029/2009JA014289)
- D.A. Gurnett, W.S. Kurth, A. Roux, S.J. Bolton, C.F. Kennel, Evidence for a magnetosphere at Ganymede from plasma-wave observations by the Galileo spacecraft. *Nature* **384**, 535–537 (1996)
- D.K. Haggerty, M.E. Hill, R.L. McNutt Jr., C. Paranicas, Composition of energetic particles in the Jovian magnetotail. *J. Geophys. Res.* **114**, A02208 (2009). doi:[10.1029/2008JA013659](https://doi.org/10.1029/2008JA013659)
- D.T. Hall, D.F. Strobel, P.D. Feldman, M.A. McGrath, H.A. Weaver, Detection of an oxygen atmosphere on Jupiter's moon Europa. *Nature* **373**, 677–679 (1995)
- D.T. Hall, P.D. Feldman, M.A. McGrath, D.F. Strobel, The far-ultraviolet airglow of Europa and Ganymede. *Astrophys. J.* **499**, 475–481 (1998)
- J.T. Hallett, D.E. Shemansky, X. Lin, A rotational level hydrogen physical chemistry model for general astrophysical application. *Astrophys. J.* **624**, 448 (2005)

- D.C. Hamilton, G. Gloeckler, S.M. Krimigis, L.J. Lanzerotti, Composition of nonthermal ions in the Jovian magnetosphere. *J. Geophys. Res.* **86**, 8301–8318 (1981)
- C.J. Hansen, D.E. Shemansky, A.R. Hendrix, Cassini UVIS observations of Europa's oxygen atmosphere and torus. *Icarus* **176**, 305–315 (2005)
- T.W. Hill, Inertial limit on corotation. *J. Geophys. Res.* **84**, 6554–6558 (1979). doi:[10.1029/JA084iA11p06554](https://doi.org/10.1029/JA084iA11p06554)
- T.W. Hill, The Jovian auroral oval. *J. Geophys. Res.* **106**, 8101 (2001)
- T.W. Hill, A.J. Dessler, F.C. Michel, Configuration of the Jovian magnetosphere. *Geophys. Res. Lett.* **1**, 3–6 (1974). doi:[10.1029/GL001i001p00003](https://doi.org/10.1029/GL001i001p00003)
- T.W. Hill, A.J. Dessler, C.K. Goertz, Magnetospheric models, in *Physics of the Jovian Magnetosphere*, ed. by A.J. Dessler (Cambridge University Press, New York, 1983), pp. 353–394
- M.E. Hill, D.K. Haggerty, R.L. McNutt Jr., C.P. Paranicas, Energetic particle for magnetic filaments. *J. Geophys. Res.* **114**, A11201 (2009). doi:[10.1029/2009JA014374](https://doi.org/10.1029/2009JA014374)
- D.E. Huddleston, C.T. Russell, G. Le, Magnetopause structure and the role of reconnection at the outer planets. *J. Geophys. Res.* **102**, 24,289–24,302 (1997). doi:[10.1029/97JA02416](https://doi.org/10.1029/97JA02416)
- W.-H. Ip, Europa's oxygen exosphere and its magnetospheric interaction. *Icarus* **120**, 317–325 (1996)
- C.M. Jackman, C.S. Arridge, Solar cycle effects on the dynamics of Jupiter's and Saturn's magnetospheres. *Sol. Phys.* **274**, 481–502 (2011). doi:[10.1007/s11207-011-9748-z](https://doi.org/10.1007/s11207-011-9748-z)
- X. Jia, R.J. Walker, M.G. Kivelson, K.K. Khurana, J.A. Linker, Three dimensional MHD simulations of Ganymede's magnetosphere. *J. Geophys. Res.* **113**, A06212 (2008). doi:[10.1029/2007JA012748](https://doi.org/10.1029/2007JA012748)
- X. Jia, R.J. Walker, M.G. Kivelson, K.K. Khurana, J.A. Linker, Properties of Ganymede's magnetosphere inferred from improved three-dimensional MHD simulations. *J. Geophys. Res.* **114**, A09209 (2009). doi:[10.1029/2009JA014375](https://doi.org/10.1029/2009JA014375)
- X. Jia, M.G. Kivelson, K.K. Khurana, R.J. Walker, Magnetic fields of the satellites of Jupiter and Saturn. *Space Sci. Rev.* **152**(1) (2010a). doi:[10.1007/s11214-009-9507-8](https://doi.org/10.1007/s11214-009-9507-8)
- X. Jia, R.J. Walker, M.G. Kivelson, K.K. Khurana, J.A. Linker, Dynamics of Ganymede's magnetopause: Intermittent reconnection under steady external conditions. *J. Geophys. Res.* **115**, A12202 (2010b). doi:[10.1029/2010JA015771](https://doi.org/10.1029/2010JA015771)
- R.E. Johnson, *Energetic Charged-Particle Interactions with Atmospheres and Surfaces*, vol. X. *Phys. Chem. Space*, vol. 19 (Springer, Berlin, 1990). 232 pp. (84 figures and 28 tables)
- R.E. Johnson, J.W. Boring, L.J. Lanzerotti, W.L. Brown, Decomposition of ice by incident charged particles: The icy satellites and Rings, in *Lunar and Planetary Institute Science Conference Abstracts*, vol. 13 (1982a), p. 366
- R.E. Johnson, L.J. Lanzerotti, W.L. Brown, Planetary applications of ion induced erosion of condensed-gas frosts. *Nucl. Instrum. Methods* **198**, 147–157 (1982b)
- R.E. Johnson, R.W. Carlson, J.F. Cooper, C. Paranicas, M.H. Moore, M.C. Wong, Radiation effects on the surface of the Galilean satellites, in *Jupiter—the Planet, Satellites and Magnetosphere*, ed. by F. Bagenal, T. Dowling, W.B. McKinnon (Cambridge University Press, Cambridge, 2004), pp. 485–512 (Chap. 20)
- S.P. Joy, M.G. Kivelson, R.J. Walker, K.K. Khurana, C.T. Russell, T. Ogino, Probabilistic models of the Jovian magnetopause and bow shock locations. *J. Geophys. Res.* **107**, 1309 (2002)
- K. Khurana, M.G. Kivelson, V. Vasylunas, N. Krupp, J. Woch, A. Lagg, B. Mauk, W. Kurth, The configuration of Jupiter's magnetosphere, in *Jupiter: Planet, Satellites, Magnetosphere*, ed. by F. Bagenal, T.E. Dowling, W.B. McKinnon (Cambridge University Press, Cambridge, 2004)
- K.K. Khurana, R.T. Pappalardo, N. Murphy, T. Denk, The origin of Ganymede's polar caps. *Icarus* **191**, 193–202 (2007)
- Y.H. Kim, J.L. Fox, The chemistry of hydrocarbon ions in the Jovian ionosphere. *Icarus* **112**, 310 (1994)
- M.G. Kivelson, D.J. Southwood, Dynamical consequences of two modes of centrifugal instability in Jupiter's outer magnetosphere. *J. Geophys. Res.* **110**, A12209 (2005). doi:[10.1029/2005JA011176](https://doi.org/10.1029/2005JA011176)
- M.G. Kivelson, K.K. Khurana, C.T. Russell, R.J. Walker, J. Warnecke, F.V. Coroniti, C. Polanskey, D.J. Southwood, G. Schubert, Discovery of Ganymede's magnetic field by the Galileo spacecraft. *Nature* **384**, 537–541 (1996)
- M.G. Kivelson, K.K. Khurana, S. Joy, C.T. Russell, D.J. Southwood, R.J. Walker, C. Polanskey, Europa's magnetic signature: Report from Galileo's pass on 19 December 1996. *Science* **276**, 1239–1241 (1997)
- M.G. Kivelson, J. Warnecke, L. Bennett, S. Joy, K.K. Khurana, J.A. Linker, C.T. Russell, R.J. Walker, C. Polanskey, Ganymede's magnetosphere: Magnetometer overview. *J. Geophys. Res.* **103**(E9), 19963–19972 (1998)
- M.G. Kivelson, F. Bagenal, W.S. Kurth, F.M. Neubauer, C. Paranicas, J. Saur, Magnetospheric interactions with satellites, in *Jupiter: The Planet, Satellites and Magnetosphere*, ed. by F. Bagenal, T.E. Dowling, W.B. McKinnon (Cambridge University Press, Cambridge, 2004), pp. 513–536
- M.G. Kivelson, K.K. Khurana, M. Volwerk, Europa's interaction with the Jovian magnetosphere, in *Europa*, ed. by R.T. Pappalardo, W.B. McKinnon, K.K. Khurana (University of Arizona Press, Tucson, 2009)

- A.J. Kliore, D.P. Hinson, F.M. Flasar, A.F. Nagy, T.E. Cravens, The ionosphere of Europa from Galileo radio occultations. *Science* **277**, 355–358 (1997)
- S. Knight, Parallel electric fields. *Planet. Space Sci.* **21**, 741–750 (1973)
- E.A. Kronberg, J. Woch, N. Krupp, A. Lagg, Mass release process in the Jovian magnetosphere: Statistics on particle burst parameters. *J. Geophys. Res.* **113**, A10202 (2008). doi:[10.1029/2008JA013332](https://doi.org/10.1029/2008JA013332)
- N. Krupp et al., Energetic particle observations in the vicinity of Jupiter: Cassini MIMI/LEMMS results. *J. Geophys. Res.* **109**, A09S10 (2004a)
- N. Krupp, V. Vasiliunas, J. Woch, A. Lagg, K. Khurana, M. Kivelson, B. Mauk, E. Roelof, D. Williams, S. Krimigis, W. Kurth, L. Frank, W. Paterson, Dynamics of the Jovian magnetosphere, in *Jupiter: Planet, Satellites, Magnetosphere*, ed. by F. Bagenal, T.E. Dowling, W.B. McKinnon (Cambridge University Press, Cambridge, 2004b)
- N. Krupp, E. Kronberg, A. Radioti, Jupiter's magnetotail, in *Magnetotails in the Solar System*, ed. by A. Keilting, C.M. Jackman, P.A. Delamere (Wiley, Hoboken, 2015). doi:[10.1002/9781118842324.ch5](https://doi.org/10.1002/9781118842324.ch5)
- W.S. Kurth, J.D. Sullivan, D.A. Gurnett, F.L. Scarf, H.S. Bridge, E.C. Sittler Jr., Observations of Jupiter's distant magnetotail and wake. *J. Geophys. Res.* **87**(A12), 10,373–10,383 (1982). doi:[10.1029/JA087iA12p10373](https://doi.org/10.1029/JA087iA12p10373)
- W.S. Kurth, D.A. Gurnett, A. Roux, S.J. Bolton, Ganymede: A new radio source. *Geophys. Res. Lett.* **24**(17), 2167–2170 (1997)
- A. Lagg, N. Krupp, J. Woch, D.J. Williams, In situ observations of a neutral gas torus at Europa. *Geophys. Res. Lett.* **30**, 110000–110001 (2003)
- F. Leblanc, R.E. Johnson, M.E. Brown, Europa's sodium atmosphere: An ocean source? *Icarus* **159**, 132–144 (2002)
- F. Leblanc, A.E. Potter, R.M. Killen, R.E. Johnson, Origins of Europa Na cloud and torus. *Icarus* **178**, 367–385 (2005)
- H. Luna, C. McGrath, M.B. Shah, R.E. Johnson, M. Liu, C.J. Latimer, E.C. Montenegro, Dissociative charge exchange and ionization of O₂ by fast H⁺ and O⁺ ions: Energetic ion interactions in Europa's oxygen atmosphere and neutral torus. *Astrophys. J.* **628**(2), 1086–1096 (2005)
- X. Ma, A. Otto, P.A. Delamere, Interaction of magnetic reconnection and Kelvin-Helmholtz modes for large magnetic shear: 1. Kelvin-Helmholtz trigger. *J. Geophys. Res. Space Phys.* **119**, 781–797 (2014a). doi:[10.1002/2013JA019224](https://doi.org/10.1002/2013JA019224)
- X. Ma, A. Otto, P.A. Delamere, Interaction of magnetic reconnection and Kelvin-Helmholtz modes for large magnetic shear: 2. Reconnection trigger. *J. Geophys. Res. Space Phys.* **119**, 808–820 (2014b). doi:[10.1002/2013JA019225](https://doi.org/10.1002/2013JA019225)
- T. Majeed, J.C. McConnell, The upper ionospheres of Jupiter and Saturn. *Planet. Space Sci.* **39**, 1715 (1991)
- M.L. Marconi, Structure and composition of Europa's atmosphere. *Bull. Am. Astron. Soc.* **35**, 943 (2003)
- B.H. Mauk, D.G. Mitchell, R.W. McEntire, C.P. Paranicas, E.C. Roelof, D.J. Williams, S.M. Krimigis, Energetic ion characteristics and neutral gas interactions in Jupiter's magnetosphere. *J. Geophys. Res.* **109**, A09S12 (2003)
- B.H. Mauk, D.G. Mitchell, R.W. McEntire, C.P. Paranicas, E.C. Roelof, D.J. Williams, S.M. Krimigis, A. Lagg, Energetic ion characteristics and neutral gas interactions in Jupiter's magnetosphere. *J. Geophys. Res.* **109**, 9 (2004)
- M.B. McElroy, The ionospheres of the major planets. *Space Sci. Rev.* **40**, 460 (1973)
- M.A. McGrath, E. Lellouch, D.F. Strobel, P.D. Feldman, R.E. Johnson, Satellite atmospheres, in *Jupiter: The planet, Satellites and Magnetosphere*, ed. by F. Bagenal, T.E. Dowling, W.B. McKinnon. Cambridge Planetary Science, vol. 1 (Cambridge University Press, Cambridge, 2004), pp. 457–483. ISBN 0-521-81808-7
- M.A. McGrath, X. Jia, K. Retherford, P.D. Feldman, D.F. Strobel, J. Saur, Aurora on Ganymede. *J. Geophys. Res.* **118**(3) (2013). doi:[10.1002/jgra.50122](https://doi.org/10.1002/jgra.50122)
- R.L. McNutt Jr. et al., Energetic particles in the Jovian magnetotail. *Science* **318**, 220 (2007)
- R.L. McNutt, J.W. Belcher, H.S. Bridge, Positive ion observations in the middle magnetosphere of Jupiter. *J. Geophys. Res.* **86**, 8319 (1981)
- F.C. Michel, P.A. Sturrock, Centrifugal instability of the Jovian magnetosphere and its interaction with the solar wind. *Planet. Space Sci.* **22**, 1501 (1974)
- G.H. Millward, S. Miller, T. Stallard, N. Achilleos, A.D. Aylward, On the dynamics of the Jovian ionosphere and thermosphere. IV. Ion-neutral coupling. *Icarus* **173**, 200–211 (2005)
- T. Miyoshi, K. Kusano, MHD simulation of a rapidly rotating magnetosphere interacting with the external plasma flow. *Geophys. Res. Lett.* **24**, 2627–2630 (1997). doi:[10.1029/97GL52739](https://doi.org/10.1029/97GL52739)
- T. Moriguchi, A. Nakamizo, T. Tanaka, T. Obara, H. Shimazu, Current systems in the Jovian magnetosphere. *J. Geophys. Res. Space Phys.* **113**, A05,204 (2008). doi:[10.1029/2007JA012751](https://doi.org/10.1029/2007JA012751)
- A.F. Nagy, A.R. Barakat, R.W. Schunk, Is Jupiter's ionosphere a significant plasma source for its magnetosphere? *J. Geophys. Res.* **91**, 351–354 (1986)

- A.F. Nagy, J. Kim, T.E. Cravens, A.J. Kliore, Hot corona at Europa. *Geophys. Res. Lett.* **22**, 4153–4155 (1998)
- F.M. Neubauer, Non-linear standing Alfvén wave current system at Io: Theory. *J. Geophys. Res.* **85**, 1171–1178 (1980)
- F.M. Neubauer, The sub-Alfvénic interaction of the Galilean satellites with the Jovian magnetosphere. *J. Geophys. Res.* **103**(E9), 19843–19866 (1998)
- J.D. Nichols, Magnetosphere-ionosphere coupling in Jupiter's middle magnetosphere: Computations including a self-consistent current sheet magnetic field model. *J. Geophys. Res. Space Phys.* **116**, A10232 (2011). doi:[10.1029/2011JA016922](https://doi.org/10.1029/2011JA016922)
- J.D. Nichols, S.W.H. Cowley, Magnetosphere-ionosphere coupling currents in Jupiter's middle magnetosphere: Dependence on the effective ionospheric Pedersen conductivity and iogenic plasma mass outflow rate. *Ann. Geophys.* **21**, 1419–1441 (2003). doi:[10.5194/angeo-21-1419-2003](https://doi.org/10.5194/angeo-21-1419-2003)
- J.D. Nichols, S.W.H. Cowley, D.J. McComas, Magnetopause reconnection rate estimates for Jupiter's magnetosphere based on interplanetary measurements at ~ 5 AU. *Ann. Geophys.* **24**, 393–406 (2006)
- A. Nishida, Reconnection in the Jovian magnetosphere. *Geophys. Res. Lett.* **10**(6), 451–454 (1983). doi:[10.1029/GL010i006p00451](https://doi.org/10.1029/GL010i006p00451)
- T. Ogino, R.J. Walker, M.G. Kivelson, A global magnetohydrodynamic simulation of the Jovian magnetosphere. *J. Geophys. Res.* **103**, 225 (1998). doi:[10.1029/97JA02247](https://doi.org/10.1029/97JA02247)
- C. Paranicas, J.M. Ratliff, B.H. Mauk, C. Cohen, R.E. Johnson, The ion environment near Europa and its role in surface energetics. *Geophys. Res. Lett.* **29**, 050000–050001 (2002)
- C. Paty, W. Paterson, R. Winglee, Ion energization in Ganymede's magnetosphere: Using multifluid simulations to interpret ion energy spectrograms. *J. Geophys. Res.* **113** (2008). doi:[10.1029/2007JA012848](https://doi.org/10.1029/2007JA012848)
- J.L. Phillips, S.J. Bame, B.L. Barraclough, D.J. McComas, R.J. Forsyth, P. Canu, P.J. Kellogg, Ulysses plasma electron observations in the Jovian magnetosphere. *Planet. Space Sci.* **41**, 877–892 (1993)
- C. Plainaki, A. Milillo, A. Mura, S. Orsini, T. Cassidy, Neutral particle release from Europa's surface. *Icarus* **210**, 385–395 (2010)
- C. Plainaki, A. Milillo, A. Mura, S. Orsini, S. Massetti, T. Cassidy, The role of sputtering and radiolysis in the generation of Europa exosphere. *Icarus* **218**(2), 956–966 (2012). doi:[10.1016/j.icarus.2012.01.023](https://doi.org/10.1016/j.icarus.2012.01.023)
- C. Plainaki, A. Milillo, A. Mura, S. Orsini, J. Saur, Exospheric O₂ densities at Europa during different orbital phases. *Planet. Space Sci.* **88**, 42–52 (2013). doi:[10.1016/j.pss.2013.08.011](https://doi.org/10.1016/j.pss.2013.08.011)
- C. Plainaki, A. Milillo, S. Massetti, A. Mura, X. Jia, S. Orsini, V. Manganò, E. De Angelis, R. Rispoli, The H₂O and O₂ exospheres of Ganymede: The result of a complex interaction between the Jovian magnetospheric ions and the icy moon. *Icarus* **245**, 306–319 (2015)
- A. Radioti, J. Gérard, D. Grodent, B. Bonfond, N. Krupp, J. Woch, Discontinuity in Jupiter's main auroral oval. *J. Geophys. Res. Space Phys.* **113**, A01,215 (2008). doi:[10.1029/2007JA012610](https://doi.org/10.1029/2007JA012610)
- L.C. Ray, R.E. Ergun, P.A. Delamere, F. Bagenal, Magnetosphere-ionosphere coupling at Jupiter: Effect of field-aligned potentials on angular momentum transport. *J. Geophys. Res.* **115**, 9211 (2010)
- L.C. Ray, R.E. Ergun, P.A. Delamere, F. Bagenal, Magnetosphere-ionosphere coupling at Jupiter: A parameter space study. *J. Geophys. Res.* **117**, A01205 (2012)
- L.C. Ray, N. Achilleos, Y.N. Yates, Including field-aligned potentials in the coupling between Jupiter's thermosphere, ionosphere, and magnetosphere. *Planet. Space Sci.* **62** (2014, submitted)
- L. Roth, Aurorae of Io and Europa: Observations and modeling. Ph.D. thesis, University of Cologne (2012). Available at <http://kups.ub.uni-koeln.de/4894>
- L. Roth, J. Saur, K.D. Retherford, D.F. Strobel, P.D. Feldman, M.A. McGrath, F. Nimmo, Transient water vapor at Europa's South pole. *Science* **343**(6167), 171–174 (2014). doi:[10.1126/science.1247051](https://doi.org/10.1126/science.1247051)
- C.T. Russell, K.K. Khurana, D.E. Huddleston, M.G. Kivelson, Localized reconnection in the near Jovian magnetotail. *Science* **280**(5366), 1061–1064 (1998). doi:[10.1126/science.280.5366.1061](https://doi.org/10.1126/science.280.5366.1061)
- J. Saur, D.F. Strobel, F.M. Neubauer, Interaction of the Jovian magnetosphere with Europa: Constraints on the neutral atmosphere. *J. Geophys. Res.* **103**, 19947–19962 (1998)
- J. Saur, P.D. Feldman, L. Roth, F. Nimmo, D.F. Strobel, K.D. Retherford, M.A. McGrath, N. Schilling, J.C. Gérard, D. Grodent, Hubble space telescope/advanced camera for surveys observations of Europa's atmospheric ultraviolet emission at eastern elongation. *Astrophysics* **738**(2), 153–165 (2011)
- F.L. Scarf, D.A. Gurnett, W.S. Kurth, R.L. Poynter, Voyager 2 plasma wave observations at Saturn. *Science* **215**, 587 (1982)
- N. Schilling, F.M. Neubauer, J. Saur, Influence of the internally induced magnetic field on the plasma interaction of Europa. *J. Geophys. Res. Space Phys.* **113**(A3) (2008)
- R.W. Schunk, A.F. Nagy, *Ionospheres*, 2nd edn. (Cambridge University Press, Cambridge, 2009)
- J.D. Scudder, E.C. Sittler, H.S. Bridge, A survey of the plasma electron environment of Jupiter—A view from Voyager. *J. Geophys. Res.* **86**, 8157–8179 (1981)
- K. Seki, A. Nagy, C.M. Jackman, F. Crary, D. Fontaine, P. Zarka, P. Wurz, A. Milillo, J.A. Slavin, D.C. Delcourt, M. Wiltberger, R. Ilie, X. Jia, S.A. Ledvina, M.W. Liemohn, B. Schunk, A review of general

- physical and chemical processes related to plasma sources and losses for solar system magnetospheres. *Space Sci. Rev.* (2015). doi:[10.1007/s11214-015-0170-y](https://doi.org/10.1007/s11214-015-0170-y)
- V.I. Shematovich, R.E. Johnson, Near-surface oxygen atmosphere at Europa. *Adv. Space Res.* **27**, 1881–1888 (2001)
- V.I. Shematovich, R.E. Johnson, J.F. Cooper, M.C. Wong, Surface-bounded atmosphere of Europa. *Icarus* **173**, 480–498 (2005)
- J.A. Slavin, E.J. Smith, J.R. Spreiter, S.S. Stahara, Solar wind flow about the outer planets: Gas dynamic modeling of the Jupiter and Saturn bow shocks. *J. Geophys. Res.* **90**, 6275–6286 (1985)
- W.H. Smyth, M.L. Marconi, Europa's atmosphere, gas tori, and magnetospheric implications. *Icarus* **181**, 510–526 (2006). doi:[10.1016/j.icarus.2005.10.019](https://doi.org/10.1016/j.icarus.2005.10.019)
- D.J. Southwood, M.G. Kivelson, R.J. Walker, J.A. Slavin, Io and its plasma environment. *J. Geophys. Res.* **85**, 5,959–5,968 (1980)
- T.S. Stallard et al., On the dynamics of the Jovian ionosphere. II. The measurements of H3+ vibrational temperature, column density and total emission. *Icarus* **156**, 498 (2002)
- N. Thomas, F. Bagenal, T. Hill, J. Wilson, The Io neutral clouds and plasma torus, in *Jupiter: Planet, Satellites, Magnetosphere*, ed. by F. Bagenal, T.E. Dowling, W.B. McKinnon (Cambridge University Press, Cambridge, 2004)
- V.M. Vasylunas, Plasma distribution and flow, in *Physics of the Jovian Magnetosphere*, ed. by A.J. Dessler (Cambridge University Press, Cambridge, 1983), pp. 395–453
- V.M. Vasylunas, A. Eviatar, Outflow of ions from Ganymede: A reinterpretation. *Geophys. Res. Lett.* **27**(9), 1347–1349 (2000)
- M.F. Vogt, The structure and dynamics of Jupiter's magnetosphere. Ph.D. thesis (2012)
- M.F. Vogt, M.G. Kivelson, K.K. Khurana, S.P. Joy, R.J. Walker, Reconnection and flows in the Jovian magnetotail as inferred from magnetometer observations. *J. Geophys. Res.* **115**, A06219 (2010). doi:[10.1029/2009JA015098](https://doi.org/10.1029/2009JA015098)
- M.F. Vogt, C.M. Jackman, J.A. Slavin, E.J. Bunce, S.W.H. Cowley, M.G. Kivelson, K.K. Khurana, Structure and statistical properties of plasmoids in Jupiter's magnetotail. *J. Geophys. Res.* **119**, 821–843 (2014). doi:[10.1002/2013JA019393](https://doi.org/10.1002/2013JA019393)
- M. Volwerk, X. Jia, C. Paranicas, W.S. Kurth, M.G. Kivelson, K.K. Khurana, ULF waves in Ganymede's upstream magnetosphere. *Ann. Geophys.* **31**, 45–59 (2013). doi:[10.5194/angeo-31-45-2013](https://doi.org/10.5194/angeo-31-45-2013)
- R.J. Walker, T. Ogino, M.G. Kivelson, Magnetohydrodynamic simulations of the effects of the solar wind on the Jovian magnetosphere (2001)
- D.J. Williams, B.H. Mauk, R.W. McEntire, E.C. Roelof, T.P. Armstrong, B. Wilken, S.M.K.J.G. Roederer, T.A. Fritz, L.J. Lanzerotti, N. Murphy, Energetic particle signatures at Ganymede: Implications for Ganymede's magnetic field. *Geophys. Res. Lett.* **24**(17), 2163–2166 (1997)
- D.J. Williams, B. Mauk, R.W. McEntire, Properties of Ganymede's magnetosphere as revealed by energetic particle observations. *J. Geophys. Res.* **103**(A8), 17,523–17,534 (1998)
- J. Woch, N. Krupp, A. Lagg, Particle bursts in the Jovian magnetosphere: Evidence for a near-Jupiter neutral line. *Geophys. Res. Lett.* **29**(7), 1138 (2002). doi:[10.1029/2001GL014080](https://doi.org/10.1029/2001GL014080)
- E.E. Woodfield, R.B. Horne, S.A. Glauert, J.D. Menietti, Y.Y. Shprits, The origin of Jupiter's outer radiation belt. *J. Geophys. Res. Space Phys.* **119**, 3490–3502 (2014). doi:[10.1002/2014JA019891](https://doi.org/10.1002/2014JA019891)
- P. Zarka, J. Queinnec, F.J. Crary, Low-frequency limit of Jovian radio emissions and implications on source locations and Io plasma wake. *Planet. Space Sci.* **49**, 1137–1149 (2001)